Characterization of TiO_2 - Water Nanofluid Droplet Evaporation

Thesis submitted towards partial fulfilment of the requirements for the award of the Degree of Master of Technology in Nano Science and Technology

By

SAPTARSHI MONDAL

Registration No: **154592** of **2020-2021**

Class Roll No: **002030701024**

Examination Roll No. **M4NST22023**

Under the guidance of **Prof. Swarnendu Sen, Prof. Apurba Kumar Santra** & **Prof. Ranjan Ganguly**

School of Material Science and Nano Technology
Jadavpur University,
Kolkata- 700032, INDIA.

August, 2022

School of Material Science and Nano Technology
Jadavpur University,
Kolkata- 700032, INDIA.

CERTIFICATE OF RECOMMENDATION

We hereby recommend that the thesis entitled as "**Characterization of TiO_2-Water Nanofluid Droplet Evaporation**", prepared by **Mr. Saptarshi Mondal** (Class Roll No: 002030701024, Registration No. 154592 of 2020-2021, Examination Roll No. M4NST22023) under our guidance, be accepted in partial fulfilment of the requirement for the award of the Degree of Master of Technology in Nano Science and Technology from the School of Material Science and Nano Technology of Jadavpur University.

_____

HOD / Director
Dr. Sourav Sarkar
Director,
School of Material Science and Nano Technology,
Jadavpur University

_____

Thesis Advisor
Dr. Swarnendu Sen
Professor,
Department of Mechanical Engineering,
Jadavpur University

_____

Thesis Advisor
Dr. Ranjan Ganguly
Professor,
Department of Power Engineering,
Jadavpur University

_____

Thesis Advisor
Dr. Apurba Kumar Santra
Professor,
Department of Power Engineering,
Jadavpur University

_____

Dean-FISLM,
Jadavpur University,
Kolkata – 700 032

School of Material Science and Nano Technology
Jadavpur University,
Kolkata- 700032, INDIA.

CERTIFICATE OF APPROVAL

The foregoing thesis titled "**Characterization of TiO_2-Water Nanofluid Droplet Evaporation**" was hereby approved by the committee of the final examination for evaluation of the thesis as a credited study of an engineering subject carried out and presented by **Mr. Saptarshi Mondal** (Class Roll No: 002030701024, Registration No. 154592 of 2020-2021, Examination Roll No. M4NST22023) in a manner satisfactory to warrant its acceptance as a prerequisite to the degree of Master of Technology in Nano Science and Technology. It was understood by this approval, the undersigned do not necessarily endorse or approve any statement made, opinion expressed or conclusion drawn therein but approve the thesis only for the purpose for which it was submitted. Committee of final examination for evaluation of thesis.

---------- ----------

---------- ----------

---------- ----------

_____ _____

Signature Date

School of Material Science and Nano Technology
Jadavpur University,
Kolkata- 700032, INDIA.

Declaration of Originality and Compliance of Academic Ethics

I hereby declare that this thesis titled " **Characterization of TiO_2 - Water Nanofluid Droplet Evaporation**" contains literature survey and original research work by the undersigned candidate, as part of my Degree of Master of Technology in Nano Science and Technology.

All Information in this document has been obtained and presented in accordance with academic rules and ethical conduct.

I also declare that, as required by these rules and conduct, I have fully cited and referenced all material results that were not original to this work.

.

Name (Block Letters): SAPTARSHI MONDAL
Class Roll No: 002030701024
Registration No: 154592 of 2020-2021
Examination Roll No. M4NST22023

_____

Signature with date

Acknowledgement

"Work" was a definition of a joint endeavour that requires togetherness not only in respect of spreading our hands towards it but also the knowledge and experience builds its foundation. In this section, I am overwhelmed in all humbleness and gratefulness to acknowledge my depth to all those who have helped me to put these ideas, well above the level of simplicity and into something concrete.

I would like to express my gratitude to my guide, Professor **Swarnendu Sen** for his strong support, patience and constant availability for technical discussions. I would like to express my particular gratitude to another guide, Professor **Ranjan Ganguly** for being my well-wisher and rendering continuous support, guidance and ideas during my thesis work. I would like to express my sincere gratitude to another guide, Professor **Apurba Kumar Santra**, for his constant patience, guidance and ideas without which completion of this thesis would have been impossible. I am grateful to all Ph.D. Scholars (A.M.R.A. Lab) and my fellow M.Tech. Researchers and Juniors I worked with for guiding me during the entire course of research work with their valuable suggestions, support and knowledge.

I would like to thank all the faculty members of **School of Materials Science & Nanotechnology, Jadavpur University, Kolkata**, for giving me the opportunity to carry out my M. Tech thesis work.

I render my heartiest thanks to the faculty members of **Department of Power Engineering, Faculty of Engineering and Technology, Jadavpur University, Kolkata** for giving me opportunity working in **Advance Materials & Research Application Lab** where I got resourceful guidance and proper research environment which has helped me to complete the thesis work more effectively and efficiently

I would like to thank my **Seniors** as well as **Juniors** from **School of Materials Science & Nanotechnology** and **Department of Power Engineering, Faculty of Engineering and Technology, Jadavpur University, Kolkata** for their moral supports throughout the duration of the thesis work.

Most of all, my deepest appreciation goes to **My Parents** for their faith, unyielding unconditional love, support, encouragement and quiet patience.

- Saptarshi Mondal

Table of Contents

Table of Figures

Abstract

Nano Science and Technology has become an emerging and impactful technology for more efficient and well-versed products in every fields. Evaporation of a droplet is common phenomena in our everyday life, it offers intriguing effects through interplay of capillary and viscous forces. Different parameters like dynamics of three phase contact line, transition of phase, generation of deposited particles patterns affects the evaporation rate. One facet of illustration of the formation of different types of patterns meets the academic quest, while the other side offers numerous applications in practical field. Investigation of post-evaporation patterns of nanoparticles suspended in a liquid droplet is increasing day by day in medical diagnosis and printing or coating technology. Nanofluids were new class of fluid made by homogeneously suspending nanometre size particles in the host liquids like water, ethylene glycol, etc. After complete evaporation of nanofluids droplet these nanometre size particles deposit on the substrate on which the droplet has been placed. Types of formation of patterns depend on many variables like types of nanoparticles, the host fluids, particles volume fraction, nature of surfactant, stabilizing time etc.

In this current experiment, TiO_2 has been chosen to synthesize nanofluids in deionized water as the base fluid. Droplets of stable suspensions of nanofluids were deposited gently on smooth, hydrophilic surfaces (cleaned glass slides). Coffee ring was created from the evaporation of TiO_2-water nanofluids droplets at volume fraction $\Phi = 0.1\%$ and $\Phi = 0.5\%$, when the parent nanofluid suspension was sonicated using bath sonicator. On the contrary, uniform patterns for $\Phi = 1.0\%$. Also, formation of coffee ring from TiO_2-water nanofluids droplet was impacted when surfactant Acetic acid (AA) and Cetyl Trimethyl Ammonium Bromide (CTAB) were added to this sample. Two types of patterns were formed by the evaporation of TiO_2-water-AA nanofluids droplet at two different volume fractions, viz., $\Phi = 0.1\%$ and $\Phi = 0.5\%$. Results, clearly indicates that deposited patterns depend on particles volume fraction. For runs where ring formation in $\Phi = 0.1\%$, Large peaks of deposited particles were noticed. There were slight high peaks in the centre part of the ring for $\Phi = 0.5\%$, indicating more concentration of nanoparticles present there. For $\Phi = 1.0\%$, peaks in intensity graph were more or less same for every area of the pattern. Average Gray value for $\Phi = 0.1\%$ was 210, for $\Phi = 0.5\%$ it was 190, for $\Phi = 1.0\%$ it was 185 as per the image analysis.

Chapter 1

1. Introduction

1.1 Motivation:

Evaporation is a natural phenomenon in our everyday life. But the mechanism of evaporation was very complex. In spite of hundreds of years of research, a lot of opportunities and challenges exists in this filed. Evaporation refers to a phase transition phenomenon that convert liquid phase into gaseous phase by absorbing heat energy. Water vaporization occurs continuously in nature and it makes water circulated between the Earth surface and sky. Liquid droplet gets vaporized when it was surrounded by unsaturated vapour. One interesting phenomenon was if liquid droplet contains some non-volatile particles, after vaporization of liquid particles non-volatile particles deposit on solid surface. This deposited pattern differs from surface to surface and liquid to liquid. The types of patterns may be of various sorts like coffee ring patterns, uniform pattern, combined patterns, stick-slip pattern, fingering structure, etc. [1] These different types of patterns have numerous applications in various field. But the problems associated to this case were sometimes uniform patterns were desired but coffee ring patterns or other patterns were formed, so qualities of the corresponding product were hampered. Therefore, researchers have tried to convert the patterns to the desired patterns. Nanofluids were new class of fluid and it was prepared by mixing nanometre size particles to the host fluid and stability of nanofluids were increased by adding proper surfactant. The deposited patterns from the evaporation of nanofluids droplet were dependent on the type of host fluid, type of nanoparticles, particles volume fraction, types of surfactant, amount of surfactant, temperature of droplet and surrounding, etc. So systematic and exhaustive experiments were necessary to observe the change of patterns and to get the desired pattern. A uniform pattern was expected for coating, inkjet printing, pesticide spray, self-assembly of nanoparticles, chip manufacturing, etc. Different size of particles contained in a droplet or cells in biomedical field can be separated by coffee ring deposition. Evaporation also plays a fundamental role in spray cooling or evaporative cooling, fuel injection, etc. Nowadays conductive and transparent coating has high demand due to its use in touch screens, OLED, LCD display and many others. Currently Indium Tin Fluoride (ITF) and Indium Tin Oxide

(ITO) were used in this field, but these were 2 very difficult to manufacture and expensive [2]. Coffee ring pattern from evaporation of droplet could solve this problem.

1.2 Nanofluids:

Nanofluids were colloidal suspension of nanometre sized material in form of particles, nanotubes, nanofibers, nanosheets, nanowires, etc., in different base fluid like engine oil, water, ethylene glycol, etc. Since the size of nanoparticles was in the range of nanometre (1-100nm), the name of the solution was nanofluids. Nanoparticles may be produced from metal, oxide and different compound. Metal such as aluminium, copper, titanium, boron, silver, etc. different metal oxide like titanium oxide, aluminium oxide, silicon oxide, copper oxide, zirconium oxide, iron oxide etc. different compound like carbon nanotube, silicon carbide, calcium carbonate, aluminium nitride etc. were used to produce nanoparticles. Now a days heat transfer phenomenon in new technology getting crucial attraction of researchers. Because high heat transfer fluid can solve many problems as day by day microprocessor being smaller and becoming powerful, so high heat transfer methodology was required to cool the microprocessor. Heat exchanger size of automobile can be reduced by using these high heat transfer fluids. Nanofluids alters the thermophysical property of base fluid due to its high surface to volume ratio such as thermal conductivity, wettability, viscosity, surface tension, etc. Introducing nanoparticles, the base fluid increases viscosity by disturbing fluid flow pattern, that have adverse effect in application of nanofluids. Nanoparticles gets stabilized in the base fluid by Brownian Motion [3]. Famed Scottish Botanist Robert Brown, in 1828 at first observed the irregular movement of suspended pollen in water, so this motion was named as Brownian motion. The movement of nanoparticles were totally random, diffusion of nanoparticles in fluid occurs by this motion and velocity of motion of particle was inversely proportional to the size of particles. So, stability of solution becomes higher as small as the size of particles. Nanofluids are widely used due to its improved properties that are relevant to engineering applications such as industrial cooling, extraction of geothermal power, automotive application like radiator coolant, lubricant etc., cooling of microchip, micro-scale fluidic application etc., and biomedical application as cancer therapeutics, nanocrysurgery etc. [4]

1.3 Literature Review:

The following section discusses some salient literature that has investigated the evaporation dynamics of nanofluid droplets. Summary of these works are provided individually.

1.3.1 Xin Zhong, Alexandru Crivoi, Fei Duan, Sessile nanofluid droplet drying, Advances in Colloid and Interface Science, Volume 217, 2015, ISSN 0001-8686:

Nanofluid droplet evaporation has gained much audience nowadays due to its wide applications in painting, coating, surface patterning, particle deposition, etc. Here the drying progress and deposition formation from the evaporative sessile droplets with the suspended insoluble solutes, especially nanoparticles were observed. The evaporation fundamental, the particle self-assembly, and deposition patterns in sessile nanofluid droplet. Both experimental and theoretical studies were presented. The effects of the type, concentration and size of nanoparticles on the spreading and evaporative dynamics were elucidated at first. The review ends with the introduction of theoretical investigations, including the Navier–Stokes equations in terms of solutions, the Diffusion Limited Aggregation approach, the Kinetic Monte Carlo method, and the Dynamical Density Functional Theory. Nanoparticles had shown great influences in spreading, evaporation rate, evaporation regime, fluid flow and pattern formation of sessile droplets. Under different experimental conditions, various deposition patterns can be formed. The existing theoretical approaches were able to predict fluid dynamics, particle motion and deposition patterns in the particular cases. On the basis of further understanding of the effects of fluid dynamics and particle motion, the desirable patterns can be obtained with appropriate experimental regulations.

- Nano fluid used here: TiO_2 and Al_2O_3
- Base fluid: Water
- Different types of patterns that were observed:
    - Coffee ring patterns
    - Uniform pattern
    - Stick slip pattern
    - Fingering structure
    - Combined pattern

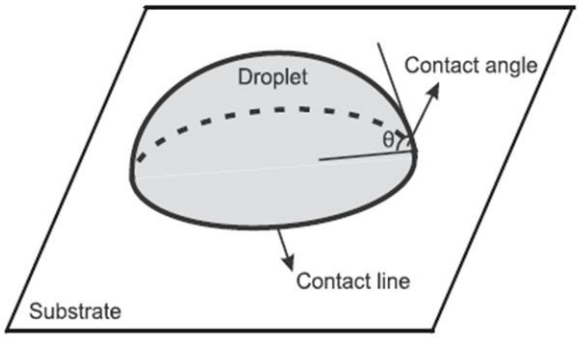

Fig. 1.3a The Contact Line and Contact Angle of a sessile droplet

- Different theoretical studies on nanofluid droplet drying
    - Navier–Stokes equations
    - Diffusion limited aggregation
    - Kinetic Monte Carlo model
    - Dynamical density functional theory.

Evolution of Al_2O_3 nanofluid droplet evaporation with sequential photographs and schematic sketches.

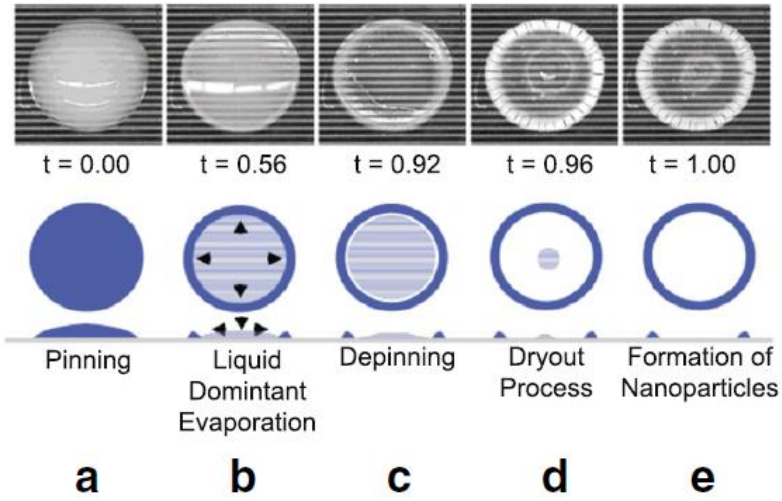

Fig. 1.3b: Evolution of Al_2O_3 nanofluid droplet evaporation with sequential images and schematic diagrams.

- Particle size: 11nm.
- Once the droplet is placed on the microheater substrate, it goes through stages of
    - (a) pinning (t=0)
    - (b) liquid dominant evaporation
    - (c) depinning (t=0.92)
    - (d) dry-out progress (t=0.96)
    - (e) formation of nanoparticles.

In below figure:

(a) Coffee Ring Pattern was observed:

- Nanoparticles: Graphite.
- Surfactant: 0.1 wt% CTAB (Cetyltri-methyl Ammonium Bromide)

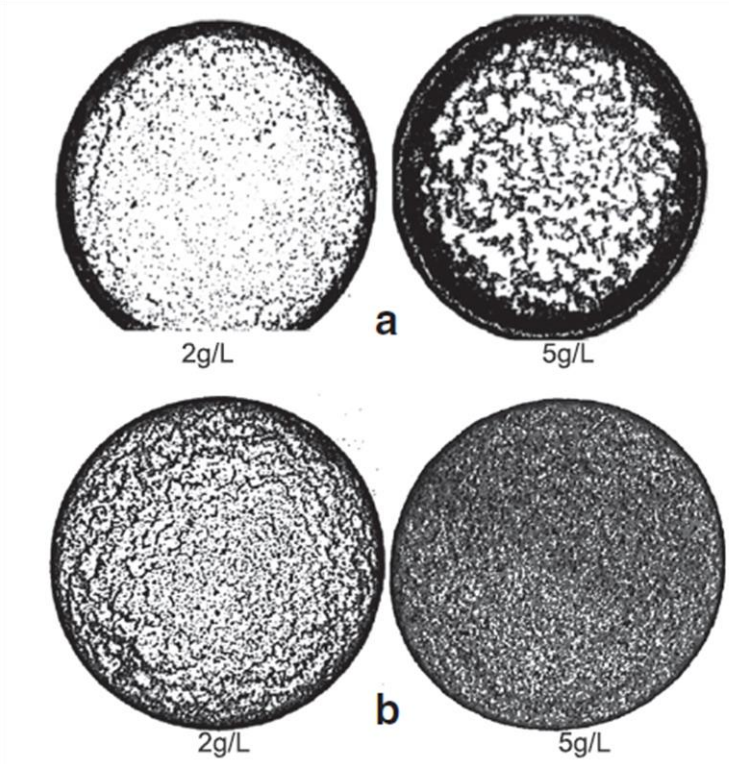

Fig. 1.3c: (a) Coffee-ring patterns from droplets with 0.1 wt% CTAB surfactant with graphite nanoparticles concentrations at 2 g/L and 5 g/L; (b) uniform patterns from droplets without surfactant with graphite nanoparticles concentration at 2 g/L and 5 g/L.

- Base fluid: Water.

(b) Uniform Pattern was observed:

- Nanoparticles: Graphite.
- Surfactant: Without Surfactant
- Base fluid: Water.

To look at the coffee ring closer, an atomic force microscopy was used to measure the width and height of ring-stains from the sessile nanofluid droplet evaporation.

In below pattern Stick-Slip Pattern was observed.

If a nanofluid droplet drying on a non-perfect surface followed the stick–slip behavior, several rings with one outside another would be left on the solid surface after the liquid was evaporated completely

- Nanoparticle: TiO_2
- Base Fluid: Ethanol

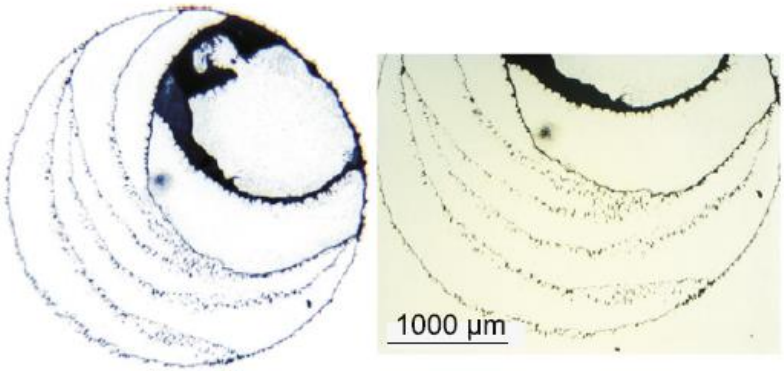

Fig. 1.3d: Stick-Slip pattern on solid surface after evaporation of ethanol droplet containing TiO_2 nanoparticles.

- No surfactant.

➢ **<u>Three Convective Mechanisms Compete to Form the Deposit</u>**

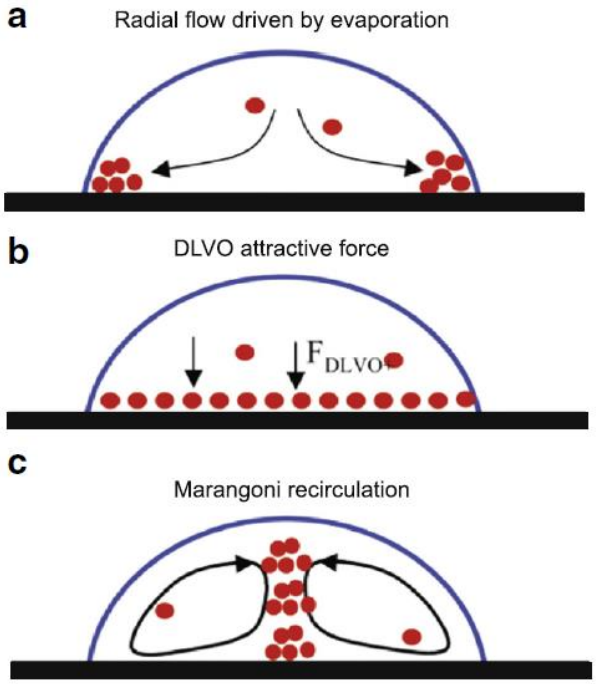

(A) A ring forms due to radial flow caused by a maximum evaporation rate at the pinned wetting line

(B) A uniform deposit forms due to an attractive DLVO force between the particles and the substrate. DLVO named after Derjaguin, Landau, Verwey and Overbeek

(C) A central bump forms due to a Marangoni recirculation loop

Fig. 1.3e: Three convective mechanisms compete to form the deposit.

➢ **<u>Navier Stokes Equation:</u>**

- There are 2 primary ways to obtain the solution (1) analytical (2) numerical
- Basically, used to the advective velocity, evaporation flux, deposit growth with time

➢ **<u>Diffusion Limited Aggregation:</u>**

- It is a process by which a fractal can be formed by solutes undergoing a random walk induced by Brownian motion in a solution.
- It is used with different models to describe particle movement and aggregation.

➢ **Dynamical Density Functional Theory:**

- Dynamical Density Functional Theory (DDFT) was applied to predict the behavior of an ultra-thin precursor film by coupling the density profile of the liquid and the nanoparticles in the nanofluids.

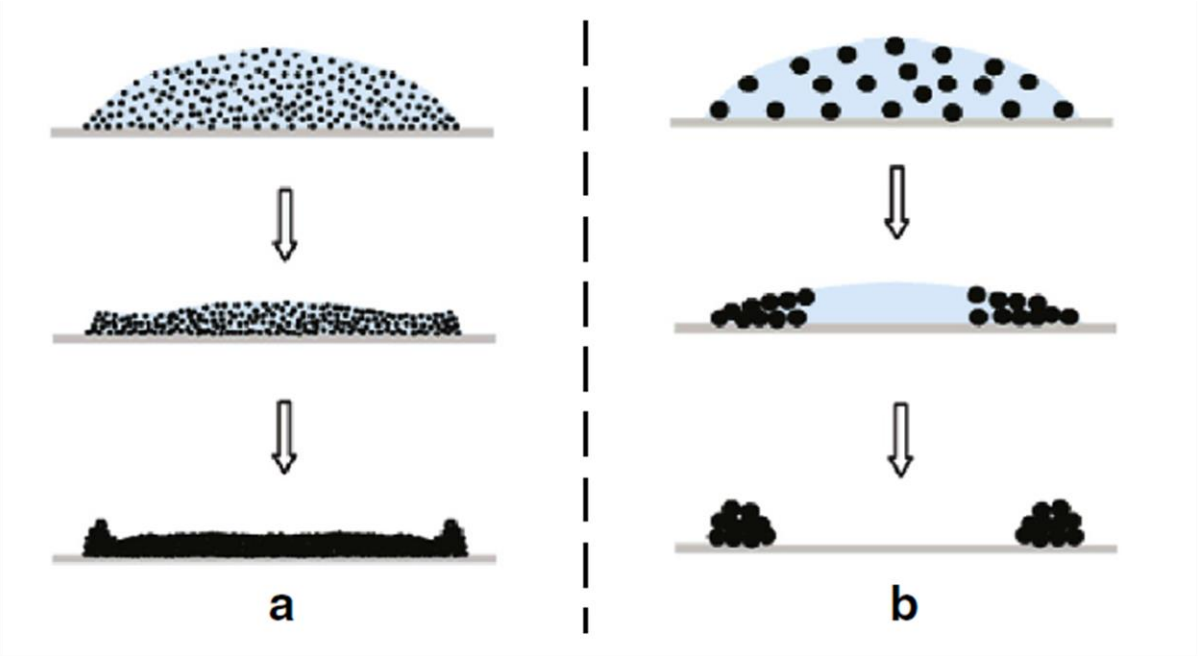

Fig. 1.3f: Schematic illustration of nanofluid droplet evaporation and dry out process depending on particle sizes: (a) a uniform distribution formed by nanoparticles with smaller size and (b) a coffee-ring pattern formed by nanoparticles with larger size.

➢ **Coffee Ring Generation:**

The coffee-ring pattern originates from the **Capillary Flow** induced by the evaporation of the drop: liquid evaporating from the edge is replenished by liquid from the interior. [5] The resulting edge ward flow can carry nearly all the dispersed material to the edge. As a function of time, this process exhibits a "rush-hour" effect, that is, a rapid acceleration of the edge ward flow at the final stage of the drying process. [6]

Evaporation induces a **Marangoni Flow** inside a droplet. The flow, if strong, redistributes particles back to the centre of the droplet. Thus, for particles to accumulate at the edges, the liquid must have a weak Marangoni flow, or something must occur to disrupt the flow. [7] For

example, **Surfactants** can be added to reduce the liquid's surface tension gradient, disrupting he induced flow. Water has a weak Marangoni flow to begin with, which is then reduced significantly by natural surfactants. [8]

Interaction of the particles suspended in a droplet with the free surface of the droplet is important in creating a coffee ring. [9] "When the drop evaporates, the free surface collapses and traps the suspended particles ... eventually all the particles are captured by the free surface and stay there for the rest of their trip towards the edge of the drop." [10] This result means that surfactants can be used to manipulate the motion of the solute particles by changing the surface tension of the drop, rather than trying to control the bulk flow inside the drop.

- **Coffee Ring Suppression:**

The coffee-ring pattern is detrimental when uniform application of a dried deposit is required, such as in printed electronics. It can be suppressed by adding elongated particles, such as cellulose fibres, to the spherical particles that cause the coffee-ring effect. The size and weight fraction of added particles may be smaller than those of the primary ones.

It is also reported that controlling flow inside a droplet is a powerful way to generate a uniform film; for example, by harnessing solute Marangoni flows occurring during evaporation. [11]

Mixtures of low boiling point and high boiling point solvents were shown to suppress the coffee ring effect, changing the shape of a deposited solute from a ring-like to a dot-like shape. [12]

Control of the substrate temperature was shown to be an effective way to suppress the coffee ring formed by droplets of water-based PEDOT: PSS solution. [13] On a heated hydrophilic or hydrophobic substrate, a thinner ring with an inner deposit forms, which is attributed to Marangoni convection. [14]

Control of the substrate wetting properties on slippery surfaces can prevent the pinning of the drop contact line, which will, therefore, suppress the coffee ring effect by reducing the number of particles deposited at the contact line. Drops on superhydrophobic or liquid impregnated surfaces are less likely to have a pinned contact line and will suppress ring formation [15] Drops with an oil ring formed at the drop contact line have high mobility and can avoid the ring formation on hydrophobic surfaces [16]

Alternating voltage electrowetting may suppress coffee stains without the need to add surface-active materials. [17] Reverse particle motion may also reduce the coffee-ring effect because

of the capillary force near the contact line. [18] The reversal takes place when the capillary force prevails over the outward coffee-ring flow by the geometric constraints.

- **Determinants of Size and Patterns:**

The lower-limit size of a coffee ring depends on the time scale competition between the liquid evaporation and the movement of suspended particles. [19] When the liquid evaporates much faster than the particle movement near a three-phase contact line, coffee ring cannot be formed successfully. Instead, these particles will disperse uniformly on a surface upon complete liquid evaporation. For suspended particles of size 100 nm, the minimum diameter of the coffee ring structure is found to be 10 μm, or about 10 times smaller than the width of human hair. The shape of particles in the liquid is responsible for coffee ring effect. [20][21] On porous substrates, the competition among infiltration, particle motion and evaporation of the solvent governs the final deposition morphology. [22]

The pH of the solution of the drop influences the final deposit pattern. [23] The transition between these patterns is explained by considering how DLVO interactions such as the electrostatic and Van der Waals forces modify the particle deposition process.

1.3.2 H.H. Lee, S.C. Fu, C.Y. Tso, Christopher Y.H. Chao, Study of residue patterns of aqueous nanofluid droplets with different particle sizes and concentrations on different substrates, International Journal of Heat and Mass Transfer, Volume 105, 2017, ISSN 0017-9310:

Main aim was to investigate the effect of both particle size and concentration on the residue pattern.

- Nanoparticles used: Al_2O_3, TiO_2
- Base liquid: Water.
- Different substrates: Glass, Stainless Steel, Teflon.

Observations:

A ring-shaped pattern was formed at low concentrations and small particle sizes for Al_2O_3 nanofluids. A uniform pattern was formed at high concentrations and large particle sizes for Al_2O_3 nanofluids. Only ring-shaped residue patterns were observed for all concentrations of TiO_2 nanofluids. In the case of different substrates, on a material with a high contact angle with water, it was difficult to form a ring-shaped pattern.

- Al_2O_3 Nanoparticle sizes of **9 nm, 13 nm, 20 nm, 80 nm and 135 nm**
- TiO_2 Nanoparticle sizes of **21 nm** in diameter
- Volume % used: **0.01, 0.05, 0.1, 0.5, 1, 2, 3 and 4.**
- Substrates used: **Glass, Stainless Steel and Teflon.**

Particle Size (nm)	Concentration (vol%)																							
	0.01			0.05			0.1			0.5			1			2			3			4		
	G	SS	T	G	SS	T	G	SS	T	G	SS	T	G	SS	T	G	SS	T	G	SS	T	G	SS	T
9	R	R	R	R	R	R	R	R	R	R	R	R	R	R	R	R	U	U	R	U	U	R	U	U
13	R	R	NO	R	R	NO	R	R	R	R	R	R	R	R	R	R	R	R	R	U	U	R	U	U
20	R	R	NO	R	R	NO	R	I	I	R	I	I	R	I	I	R	I	I	R	I	I	R	U	U
80	R	R	R	R	R	R	R	I	R	R	I	R	R	U	I	R	U	U	R	U	U	R	U	U
135	R	R	NO	R	R	R	R	R	R	R	R	U	R	U	U	U	U	U	U	U	U	U	U	U

Fig. 1.3g: Summary of the residue patterns on different materials of substrates and nanoparticles of AL_2O_3 nanofluid. "G", "SS" and "T" denote different materials of substrates, glass, stainless steel and Teflon accordingly, for different patterns, "R", "I", "U" and "NO" represent ring-shaped, irregular, uniform and not observable, respectively.

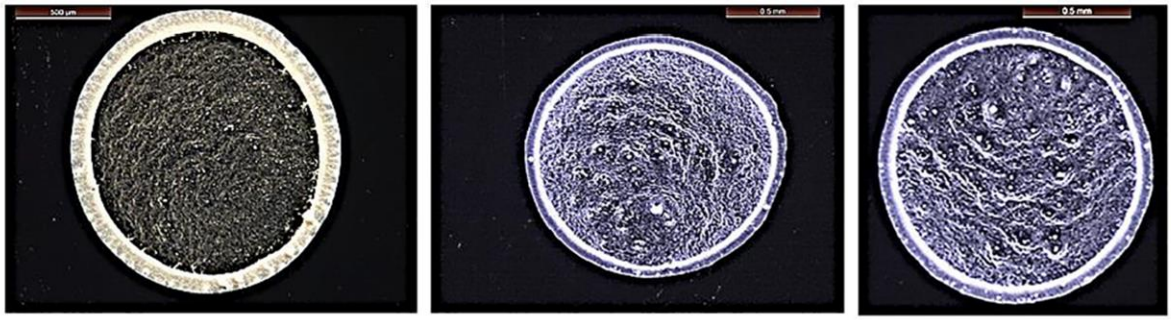

Fig. 1.3g: Pattern of three trials of the experiments of 0.01 vol% 9nm Al_2O_3 nanofluid.

In Fig. 1.3g it was observed that patterns of three trials of the experiments of 0.01, volume fraction of 9 nm Al_2O_3 Nanofluid.

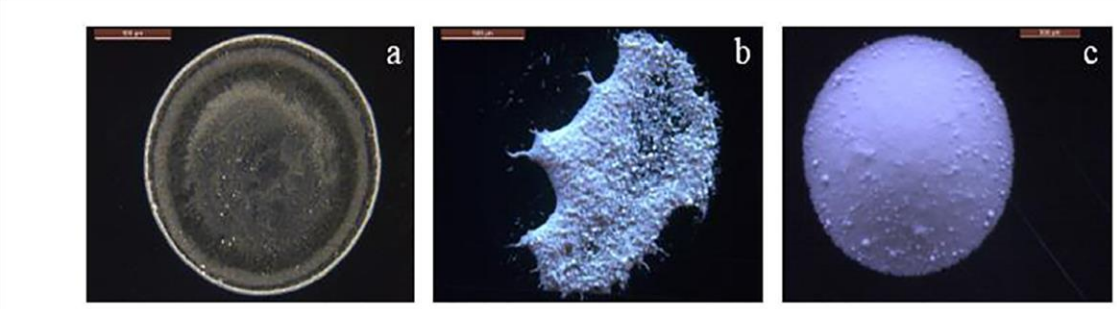

Fig. 1.3h: Comparison of the residue patterns of Al_2O_3 nanofluids in different particle sizes and concentrations (a) 9 nm 0.01 vol%, (b) 80 nm 0.5 vol% and (c) 135 nm 4 vol% on stainless steel. The scale bar is 500µm.

In Fig. 1.3h, it was observed that there was a clear ring generation for (a) Al_2O_3 nanofluid for particle size and concentration 9 nm 0.01% volume. And other deformed pattern generation for

Fig. 1.3i

(b) 80 nm 0.5% vol% and (c) 135 nm 4 vol% on stainless steel substrate. The scale bar is 500μm.

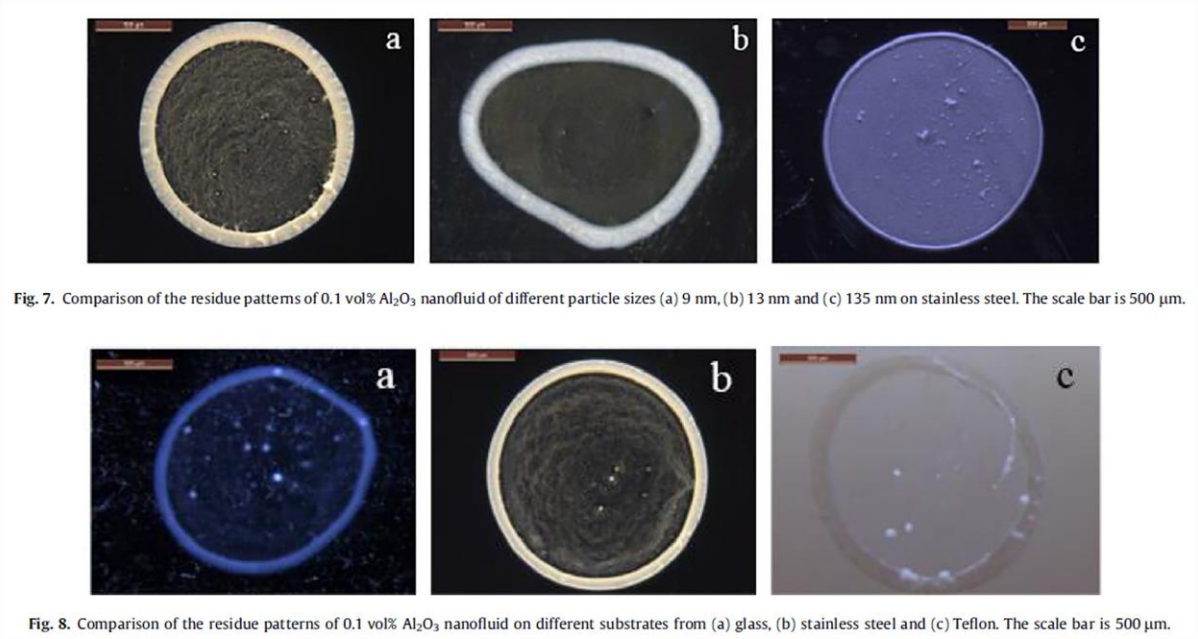

Fig. 1.3i: First row: Comparison of the residue patterns of Al_2O_3 nanofluids in different particle sizes (a) 9 nm, (b) 13 nm and (c) 135 nm on stainless steel. The scale bar is 500μm.

Second row: Comparison of the residue patterns of 0.1 vol% Al_2O_3 nanofluid on different substrates from (a) glass, (b) stainless steel and (c) Teflon. The scale bar is 500μm

In Fig. 1.3i first row of patterns are the comparison of 0.1 vol% Al_2O_3 nanofluid of different particle sizes (a) 9 nm, (b) 13 nm, and (c) 135 nm of stainless steel. The scale bar is 500 μm. For second row those are comparison of the residue patterns of 0.1 vol% Al_2O_3 nanofluid on different substrates from (a) glass, (b) stainless steel and (c) Teflon. The scale bar is 500 μm.

1.4 Gap Area:

Lot of experiments have been performed to understand the behaviour of droplet evaporation till date, but very few experiments have been carried out on droplet evaporation particularly regarding TiO_2-water nanofluids sessile droplet evaporation on glass substrate with CTAB and Acetic Acid (AA) surfactants. Depicting the deposit patterns during and after the evaporation of the nanofluid-droplets was the primary aim of this thesis. In many areas, uniform patterns were desired but coffee ring patterns were formed instead. So, researchers try to suppress this coffee ring patterns, and promote the formation of uniform patterns. Nevertheless, the research coverage in this area were still in a fledgling stage. Many researchers proposed contradicting results in the production of evaporation pattern. As Yunker et al. [24] proposed that type of deposition pattern depends on 2.0 aspect ratio of particles size, but Bhardwaj et al. [25] proposed that particles aspect ratio do not have any effect on the formation of deposition patterns and it totally dependent on the DLVO interaction that can be varied by changing pH value. The present thesis attempts to resolve these dichotomies and characterize the deposit patterns for a few specific nanofluid samples.

1.5 Objectives:

The objectives of current experiment were as follows:

- To prepare TiO_2-water nanofluids with 0.1%, 0.5% and 1.0% volume fraction using bath-sonication.
- To prepare TiO_2-water nanofluids with surfactant CTAB and Acetic Acid (AA), 0.5% and 1.0% volume fraction using bath-sonication.
- To describe the post-evaporation particle deposition patterns of surfacted- and non-surfacted nanofluids for 0.1%, 0.5% and 1.0% volume fraction.
- To describe the effect of the type of surfactant on the post-evaporation deposit pattern.
- To describe the effects of droplet size on the deposit pattern,
- To analyse Gray Intensity Graphs of patterns after evaporation and determine peak values.
- To analyse contact angle of the deposited droplets on the glass slides.

2. Materials and Methods:

2.1 List of Equipment and Materials Used:

2.1.1 Equipments Used:

- High Accuracy Electric Weight Balance Machine (Sartorius, BSA 224S – CW, max 220g, accuracy 0.1mg)
- Optical Microscope – High Accuracy Optical Microscope with up to 4.5x zoom (Magnus, MSZ – TR, 220 – 240V, 0.2A, 50 – 60 Hz, No.: 16G0951)
- Goniometer – High Accuracy Contact Angle Measurement Tool (High performance aberration corrected imaging lens with precise manual focus adjustment. Dimension - 500 x 400 x 498 mm. Power supply - 230VAC, 50 Hz)
- Bath Sonicator – (Model – USB 3.5L H DTC, Serial No. – 369 APR 2017, Supply volt – 230V AC 50Hz)
- Medical syringe – Dispovan medical syringes.
- Micro Pipette – 1 to 10 μL.
- Blue needle – 0.41mm diameter, volume - 15.1 μL.
- Magnetic stirrer – (REMI, 2MLH)
- Magnetic stirrer rods - The small one (3cm length)
- Measuring cylinder – Borosilicate Glass
- Lab glass bottles – Borosilicate Glass
- Microscopic Scale Bar.

2.1.2 Materials Used:

- TiO_2 Nanoparticles (Sigma Aldrich) of average size in diameter 21 nm
- Distilled Water (Merck Millipore) with purity 99.7%
- Surfactant 1 – Cetyltrimethylammonium Bromide (CTAB), (SRL) Extra pure AR, Powder Form, 99% purity.
- Surfactant 2 – Acetic Acid (Emplura) 99 – 100%, M = 60.05g/mol, 1L = 1.05 kg, Liquid Form, 99% purity.
- Acetone (Fisher Scientific) CAS No.: 67 – 64 – 1, $(CH_3)_2CO$ = 58.08, Prod. No.: 3351C, 99% purity.

2.2 Nanofluid Synthesis:

Researchers produced advanced heat transfer fluid that were known as nanofluids by dispersing the nano-meter sized material into the base fluid which has lower thermophysical property like thermal conductivity, viscosity, thermal diffusivity, etc. Maxwell [26], in 1873 first proposed the technique of enhancing thermal conductivity of fluid by mixing solid particles, but this technique failed to achieve the attention of researchers due to different troubles such as erosion, clogging and sedimentation during the flow. Later Masuda et al., in the year of 1993, followed up the study of Maxwell and became able to prepare the new class of fluid with high thermal conductivity, but sedimentation of particle into the fluid reduces the performance of solution. Choi in 1995, came on step forward and produced advanced heat transfer fluid that were known as nanofluids by diffusing nanometre sized particle into the base. Produced fluid exhibited better performances without showing significant stability problem.

Millimetre and Micrometer sized particle could not achieve the better performance because of particle clogging, corrosion of components, excessive pressure drops, particle sedimentation, etc. This problem was overcome by dispersing nanometre sized particle into the base fluid with desirable volume fraction. Producing homogeneous and stable mixture of nanoparticles and base fluid was the most vital issue for preparing nanofluids because it was not simple mixture of two component. For better performance of nanofluids, agglomeration free homogeneous suspension of nanoparticles in the base fluid was required. Two methods were mainly used for the preparation of nanofluids:

I) Single or One-step method and

II) Two-step method

In this experiment Two-Step Method is used.

Two Step Method:

This method was widely used to prepare nanofluids. There were two steps in this method. Nanorods, nanoparticles, nanosheets, nanofibers, nanotubes, etc., were prepared in dry powder form in first step by hydrothermal synthesis, sol-gel method, microemulsion, etc. Then in the second step, the produced nanoparticles were dispersed into the base fluid by magnetic force agitation, ball milling, ultrasonic agitation, high shear mixing etc.

In this experiment was done in Two–Step Method. After weighing the nano particles it was then added into the lab glass bottles containing water, and first stirred with hands for a while, then it was put on Magnetic Stirrer (Fig. 2.2b) for mixing for 2 hours. Magnetic Stirrer

Rod (3cm, smaller one) was used for stirring. After 2 hours, the solution was then Bath Sonicated for 2 more hours for homogeneous mixing. Sonicator was used to agitate particles in a solution. It converts an electrical signal into a physical vibration to break substances apart. These disruptions can mix solutions.

2.2.1 Nanoparticle Measurement:

Amount of Nanoparticle to be used was measured by using the Volume Fraction Equation (1). Where, Φ = Volume Fraction of the desired solution,

$$\Phi = \frac{\left(\frac{w}{\rho}\right)nanoparticles}{\left(\frac{w}{\rho}\right)nanoparticles + \left(\frac{w}{\rho}\right)water} \quad \ldots\ldots(1)$$

w = weight of the water / nanoparticles. ρ = density of the water / nanoparticles. Here 3 volume fractions were used 0.1%, 0.5% and 1.0%. An electric balance (Fig. 2.2a) with excessive accuracy (Sartorius, BSA 224S – CW, max 220g, accuracy 0.1mg) was utilized to weigh the amount of surfactants and nanoparticles. The electric balance machine was kept on for 45 mins to stabilize before using it. Weighing of nanoparticles was done on a butter paper so that any amount of nanoparticle wouldn't stick to the paper when it was added into the water.

Fig 2.2a. Electronic Balance

2.2.2 Mixing & Sonication:

The mixing of the solution was done in Two–Step Method. After weighing the nano particles it was then added into the lab glass bottles containing water, and first stirred with hands for a while, then it was put on Magnetic Stirrer (Fig. 2.2b) for mixing for 2 hours. Magnetic Stirrer Rod (3cm, smaller one) was used for stirring. After 2 hours, the solution was then Bath Sonicated for 2 more hours for homogeneous mixing. Sonicator was used to agitate particles in a solution. It converts an electrical signal into a physical vibration to break substances apart. These disruptions can mix solutions.

Fig 2.2b. Magnetic Stirrer

➢ **With Surfactant:**

In this case, Surfactant was first mixed with water. The ratio was taken as 1:10 = Surfactant: Nanoparticles. For CTAB it was easy to measure as it was in powder form. But Acetic Acid (AA) was in liquid form, so after calculating the ratio amount (1:10), amount of weight was converted into relevant amount of volume using, $\rho = m / v$, and Micro Pipette was

(a (b) (c

2.2.2a: (a) TiO_2 Powder (b) CTAB (c) Acetic Acid (AA)

used to measure that volume. After measuring the proper amount of surfactant, it was then added into the water and mixed for 2 hours on Magnetic Stirrer. After stirring then Nanoparticles were added and stirred again for 2 hours. After mixing then the solution was Bath Sonicated for 2 hours again for homogeneous mixing. There was a tendency of precipitation after 1 week of Nanofluid preparation so its better to perform the experiment within 1 week of Nanofluid preparation for better and accurate results.

Table 2.2: Summary of Nanofluid Synthesis:

➢ Table 2.2a: Without Surfactant:

Contents	Density (ρ) (Kg/m^3)	Used amount in experiment	Weight (w) (gm)	Volume fraction for nanoparticles (Φ) (%)	Rpm when it's stirred	Everyday sonication	Volume of droplet (µL) (For blue needle)
Water	1000	20 ml	23.6				
TiO_2 (21 nm)	4260	---	0.0022	0.1	600	160 min	15.1
TiO_2 (21 nm)	4260	---	0.0110	0.5	600	60 min	15.1
TiO_2 (21 nm)	4260	---	0.0220	1.0	600	60 min	15.1

➢ Table 2.2b: For CTAB:

Contents	Density (ρ) (Kg/m^3)	Weigh t (w) (gm)	Volume fraction for nanoparticles (Φ) (%)	Rpm when it's stirred	Everyday sonication	Volume of droplet (µL) (For blue needle)	Surfactant (gm)
TiO_2 (21 nm)	4260	0.0110	0.5	600	60 min	9.23	0.0011
TiO_2 (21 nm)	4260	0.0220	1	600	60 min	9.23	0.0022

➢ Table 2.2c: For Acetic Acid (AA):

Contents	Density (ρ) (Kg/m^3)	Weight (w) (gm)	Volume fraction for nanoparticles (Φ) (%)	Rpm when it's stirred	Everyday sonication	Volume of droplet (µL) (For blue needle)	Surfactant (µL)
TiO_2 (21 nm)	4260	0.0110	0.5	600	60 min	8.17	1.5 µL
TiO_2 (21 nm)	4260	0.0220	1	600	60 min	8.17	2.1 µL

(d) (e) (f)

2.2.2b: (d) TiO_2 Water (0.1%, 0.5%, 1.0%) (e) TiO_2 Water CTAB (0.5%, 1.0%) (f) TiO_2 Water AA (0.5%, 1.0%)

2.2.3 Experimental Setup & Procedure:

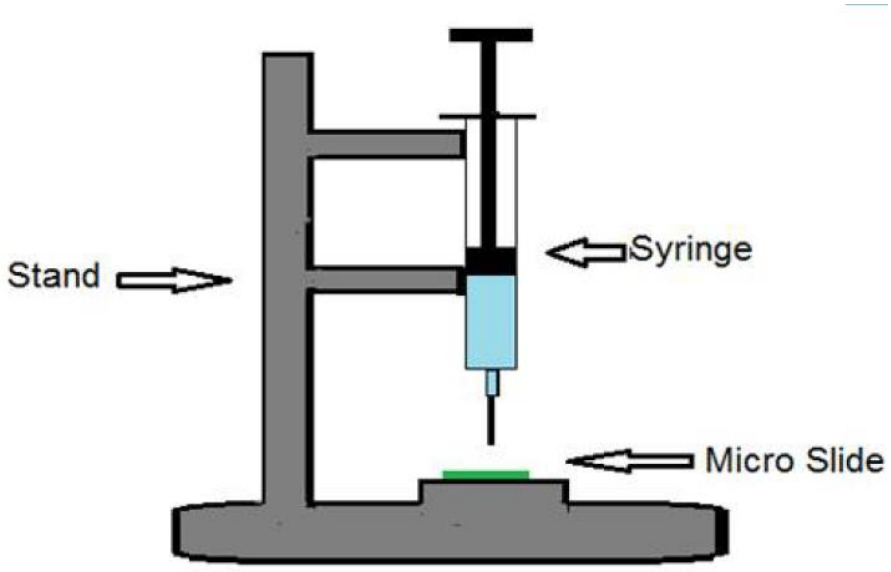

2.2.3a: Experimental Setup

An experimental set up was made, the set up was very simple, was shown schematically in above figure. At first a metallic retort stand was collected, then two clamps were attached to the retort stand. A simple modification was done of clamp so that a syringe can be attached to the clamp rigidly and syringe can be changed easily. Droplet was deposited on the glass micro slide by directly pressing the plunger of medical syringe by finger. Before the deposition of droplet on the micro slide, the micro slide was cleaned and rinsed properly to remove any dust particle already deposited on the micro slide. To clean the micro slide, at first it was rinsed in acetone, then it was ultrasonicated in bath sonicator by submerging it into acetone for 5 minutes. Then it was sonicated for another 5 minutes in bath sonicator by submerging it into distilled water. After that the microslide was wiped well by tissue paper. Then it was air dried well with hot air to make all water particles evaporate. Then micro slide was placed on a horizontal platform that was enclosed from the side with a cardboard box to prevent air-current and radiative heat influx. A syringe containing the nanofluid under investigation was mounted vertically atop the glass slide with a gap of ~5 mm between the tip of the needle and the glass slide. To dispense the nanofluid, the plunger of the syringe was pressed by finger slowly, so that only one drop of nanofluid deposited on the glass micro slide.

Fig 2.2c. Bath Sonicator

Then the slide was kept in the same position inside the cardboard box for a duration of approximately 45 mins to 90 mins (varies for different volume fractions) so that all the water got evaporated and a deposition pattern of nanoparticles were formed.

Fig 2.2d. Magnetic Stirrer

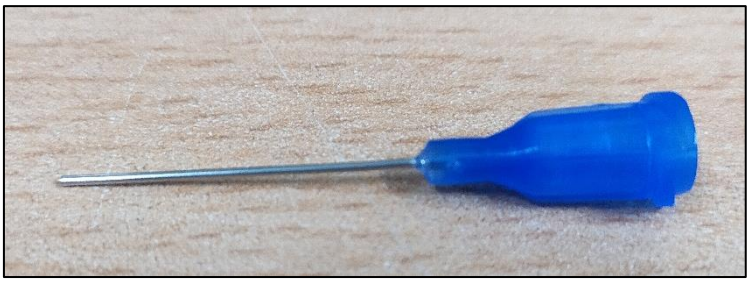

Fig 2.2e. Blue Needle

Each experiment was repeated for 9 times for each volume fractions (0.1%, 0.5%, 1.0%) to verify the observation against experimental uncertainties. Size of the generated droplets were controlled by using one type of needle i.e. blue needle (inner diameter = 0.41 mm) dispensed 15.1 μL of the nanofluid. For surfacted samples of TiO_2 samples, the dispensed volumes differed, since the surface tension of the liquid differed depending upon the surfactant.

➢ **Table 2.2d: Dispensed Volume of Droplets for Different Solutions:**

Solution (Φ = 0.1%, 0.5%, 1.0%)	Volume (μL)
TiO_2 – Water	15.1
TiO_2 – Water – CTAB	9.23
TiO_2 – Water – AA	8.17

Fig 2.2f. Microscopic Scale Bar

Then after evaporation the micro slide with deposition pattern of nanoparticles were observed under Optical Microscope (Fig 2.2g) at 1.5x zoom. It was connected to desktop and Magvision software was used. The image was calibrated for its relevant length scale against a calibration scale. A Microscopic Scale Bar (Fig 2.2f) was used so that the actual size of deposition pattern could be reported by using it as reference. ImageJ software was used to scale the image patterns of every droplets.

After getting the images of pattern, then those were analysed again in ImageJ software, and Colour Intensity Graphs were plotted against a line passing through centre of the pattern at 4 different angles i.e. 0^0, 45^0, 90^0, 135^0.

Contact angles were measured using Goniometer. (Fig 2.2h) Nanofluid droplets were taken in Micro – litre Syringe and dispensed on glass microslide using high precision mechanical dispense system provided in the system. The system was connected to a desktop where a software was present named as Contact Angle Measurement Tool. It was used to analyse the contact angle of each droplets.

Fig 2.2g. Optical Microscope

Fig 2.2h. Goniometer for contact angle measurement

2.3 Image Analysis:

After the evaporation of nanofluid droplets, pattern was observed. The pattern was then captured under optical microscope for further analysis. The microscope zoom was fixed to 1.5x zoom for image capturing. The tool used here for advance analysis was 'Image J'. Firstly, one microscopic scale bar was used while capturing the image, for scaling the image later in Image J. Then the scale bar in the image was set using the reference scale and initially the width, height and diameter of the generated ring was measured for volume fraction, $\Phi = 0.1\%$, $\Phi = 0.5\%$ and $\Phi = 1.0\%$. Now for $\Phi = 0.1\%$ and $\Phi = 0.5\%$ ring pattern was found (Fig. 1, Fig. 20), where the ring diameter in $\Phi = 0.1\%$ (approx. 0.2 to 0.6 mm) was greater than the ring diameter of $\Phi = 0.5\%$ (approx. 0.02 to 0.1 mm) ring patterns. Uniform pattern was observed for $\Phi = 1.0\%$, so only normal height and width of the pattern was measured for that volume fraction. For TiO_2-water volume fraction of $\Phi = 0.5\%$ with CTAB surfactant, ring pattern was observed of diameter varies form ~0.1 mm to ~0.12 mm in thickness. For TiO_2-water volume fraction of $\Phi = 1.0\%$ with CTAB surfactant, very thin ring pattern was observed of diameter varies form ~0.02 mm to ~0.06 mm in thickness. For TiO_2-water volume fraction of $\Phi = 0.5\%$ with Acetic Acid (AA) surfactant, an interesting ring pattern was noticed. Similar to a flower like shape. For TiO_2-water volume fraction of $\Phi = 1.0\%$ with Acetic Acid (AA) surfactant, uniform pattern was found. No ring patterns were formed.

3. Results and Discussions:

Table 3: Experiment Results/Datas:

Table 3a: Droplet Pattern Datas:

Type of Nanofluid	Volume fraction (Φ)	Droplet volume (μL)	Pattern width (mm)	Pattern height (mm)	Generated Ring thickness (mm)
TiO_2 - Water	0.1	15.1	5.055	5.446	0.2-0.6
TiO_2 - Water	0.5	15.1	5.698	5.69	0.07-0.1
TiO_2 - Water	1.0	15.1	6.396	5.791	Uniform
TiO_2 – Water CTAB	0.5	9.23	5.158	5.376	0.1-0.12
TiO_2 – Water CTAB	1.0	9.23	6.202	6.222	0.02-0.06
TiO_2 – Water AA	0.5	8.17	1.031	1.041	---
TiO_2 – Water AA	1.0	8.17	4.56	4.774	Uniform

Table 3b: Gray Values for Different Angles:

Type of Nanofluid	Volume fraction (Φ)	0 Degree		45 Degree		90 Degree		135 Degree	
		Left Peak	Right Peak	Left Peak	Right Peak	Left Peak	Right Peak	Left Peak	Right Peak
TiO_2 - Water	0.1	210	220	210	210	210	210	210	205
TiO_2 - Water	0.5	190	181	195	195	195	190	190	181
TiO_2 - Water	1.0	183		185		187		185	
TiO_2 – Water CTAB	0.5	220	215	220	210	215	215	210	220
TiO_2 – Water CTAB	1.0	185		185		185		182	
TiO_2 – Water AA	0.5	110	110	100	110	110	100	100	100
TiO_2 – Water AA	1.0	180		180		180		180	

Table 3c: Contact Angles:

Type of nanofluid	Volume fraction (Φ)	Left Contact Angle (^{0})	Right Contact Angle (^{0})
TiO_2 - Water	0.1	59.82	60.68
TiO_2 - Water	0.5	58.97	59.82
TiO_2 - Water	1.0	60.68	61.20
TiO_2 – Water CTAB	0.5	61.54	62.4
TiO_2 – Water CTAB	1.0	63.26	65.84
TiO_2 – Water AA	0.5	62.92	64.98
TiO_2 – Water AA	1.0	59.82	60.68

3.1 Nanofluid Without Surfactant:

As mentioned in Section 2, sessile droplet evaporation experiments were performed by depositing microliter volumes droplets of nanofluids on clean glass surfaces and observing the particle deposition patterns under the microscope after the droplets were allowed to evaporate in a quiescent environment. Table 3 summarizes the salient deposit attributes (viz., pattern height, width, ring thickness, etc.) for different particle volume fractions and surfactant combinations. The contact angle data for the experimental runs are also summarized in Table 3c.

3.1.1 Pattern Analysis:

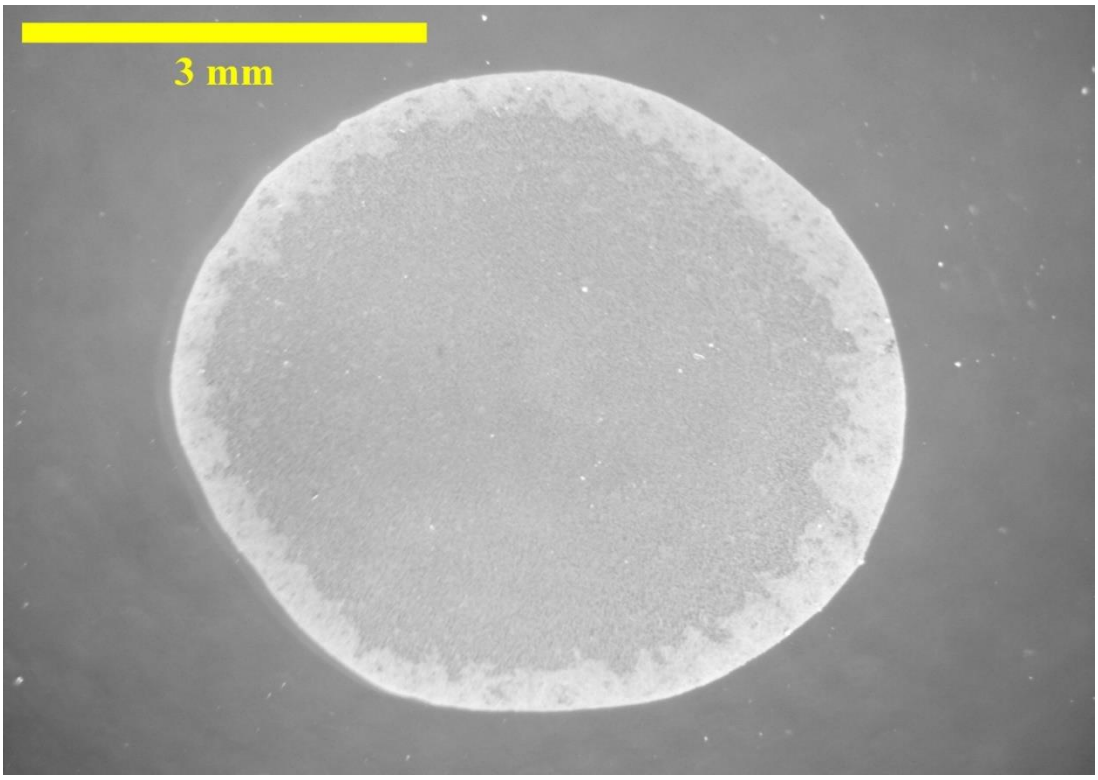

Fig 3.1: TiO_2 – Water Nanofluid after evaporation droplet pattern (Φ=0.1%) deposited on Glass Substrate. Volume ~15.1 µL. Droplet Pattern Width: ~5.446 mm, Height: ~5.055 mm. Generated Ring varies from ~0.2 mm to ~0.6 mm in thickness

As per experimental procedure, TiO_2 – water nanofluids were prepared and used for droplet deposition procedure for 3 particular volume fractions (0.1%, 0.5%, 1.0%) taken 9 times for each volume fraction. Different uniform and ring patterns were observed. Also, separate colour intensity graphs and contact angles were measured of each droplets of different volume fractions. In fig. 1, **for Φ=0.1%,** a non-homogeneous nanoparticle deposition was seen around the periphery of the evaporated droplet pattern. Also, slight uniform deposition was seen in the middle of evaporated droplet pattern. **Generated Ring varies from ~0.2 mm to ~0.6 mm in thickness. Droplet pattern width was measured ~5.446 mm, and height: ~5.055 mm.** The generation of coffee ring pattern was explained by Deegan et al. [27]. They proposed that radially outward flow was generated during evaporation of droplet, as evaporation rate was maximum at three phase contact line, so to fill up the loss of liquid particles this radially outward flow was generated. This coffee ring patterns were seen by many researchers [28], [29]. Shen et al. [30] showed that competition occurred between evaporation rate and velocity of particles movement to produce post evaporation patterns. If the rate of droplet evaporation was too fast suspended particles get deficient time to move to the periphery. So, the chance of

formation of coffee ring decreases. They showed that there should be lower limit for the size of droplet to generate coffee ring. For 100 nm particles size, the droplet size was estimated to be 10 μm. Nguyen et al. [31] proposed that evaporation of nanofluids droplet increased the rate of evaporation compared to base fluid due to formation of coffee ring, as evaporation rate depends on peripheral length three phase contact line. They used aqueous organic pigment droplet on smooth silicon wafers substrate. In Fig. 2, for Φ=0.5% a very thin line of nano particle deposition at the periphery was observed, where the generated Ring varies from ~0.07 mm to ~0.1 mm in thickness. Droplet pattern width measured ~5.698 mm, and height ~5.690 mm. In this case a gradual flow of nanoparticle deposition towards centre due to Marangoni flow was noticed. As evaporation rate was maximum at three phase contact line, capillary convection induces radially outward flow that carries nanoparticles and surfactant molecules towards the three-phase contact line. So, concentration of surfactant at three phase contact line increases compared to another portion of droplet. As surface tension decreases with the increase of surfactant concentration, surface tension gradient was produced in the droplet, which in turn creates Marangoni flow. The latter drives the particles radially inward, that was opposite to the outward capillary convection. This suppresses the formation of coffee ring toward the latter part of evaporation and the deposit pattern showed gradient distribution towards the centre.

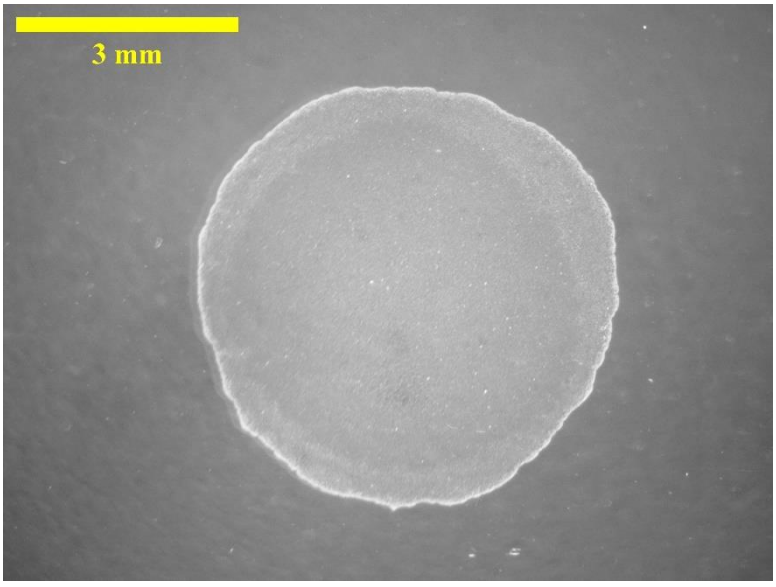

Fig 3.2: TiO_2 – Water Nanofluid after evaporation droplet pattern (Φ=0.5%) deposited on Glass Substrate. Volume ~15.1 μL. Droplet Pattern Width: ~5.698 mm, Height: ~5.690 mm. Generated Ring varies from ~0.07 mm to ~0.1 mm in thickness

In Fig. 3, for Φ=1.0% uniform pattern was observed here. Droplet pattern width measured ~6.396 mm, and height ~ 5.791 mm. Shimoni et al. in 2014, [32] showed an interesting application of coffee ring patterns. Flexible and transparent conductors were very essential element now a days because it was considerably used in various devices like solar cells, displays, touch screen in smart phone etc. Indium Tin Fluoride, Indium Tin Oxide etc. were used as a conductive transparent coating. But these were very costly and much difficult to produce. If a thin metallic wire mesh was fused onto glass sheet, it becomes a possible alternative. But some problems arise here also, such as conductive wire becomes visible and decreases transparency. These problems can be overcome by depositing coffee ring patterns of conductive particles like carbon nanotube (CNT), silver nanoparticles etc. on the transparent substrate. Perpendicular arrays were generated by to form connected network by ink jet printing technique. The ring spacing and thickness needs to be calculated to optimize conductivity and transparency. Wong et al. [33] used coffee ring pattern to separate cell based on the size of cells, smaller cell deposited close to the three-phase contact line.

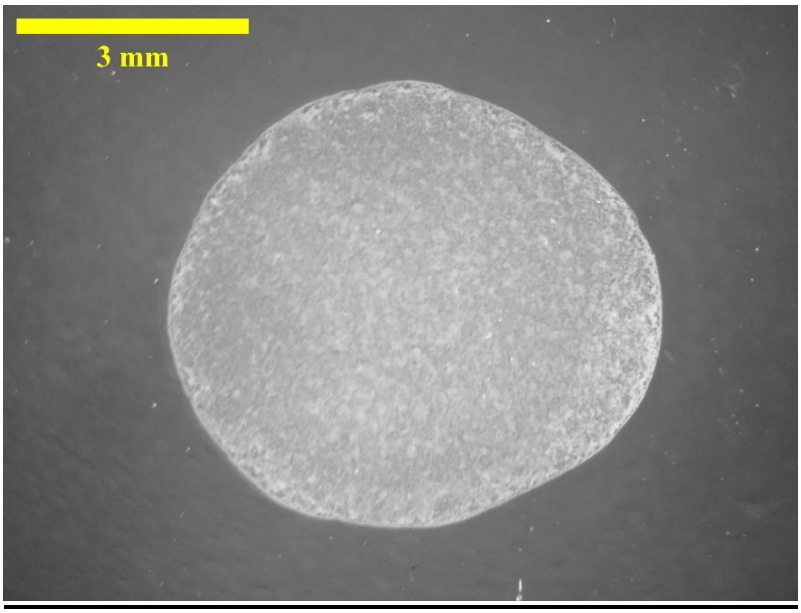

Fig 3.3: TiO_2 – Water Nanofluid after evaporation droplet pattern (Φ=1.0%) deposited on Glass Substrate. Volume ~15.1 µL. Droplet Pattern Width: ~6.396 mm, Height: ~ 5.791 mm. uniform pattern was noticed

3.1.2 Contact Angle Analysis:

Analysing the results of the Contact angles for Φ=0.1%, Φ=0.5% and Φ=1.0%, there isn't much difference in right angle and left contact angles in Φ=0.1% and Φ=0.5%, for Φ=0.1% (Fig. 4) left angle measured as 59.82^0 and right angle measured as 60.68^0. Similarly, for Φ=0.5% (Fig.

5) left angle measured as 58.97^0 and right angle measured as 59.82^0. but there was a slight difference in angles for Φ=1.0%, (Fig. 6) where left angle was measured as 60.68^0 and right angle measured as 61.20^0

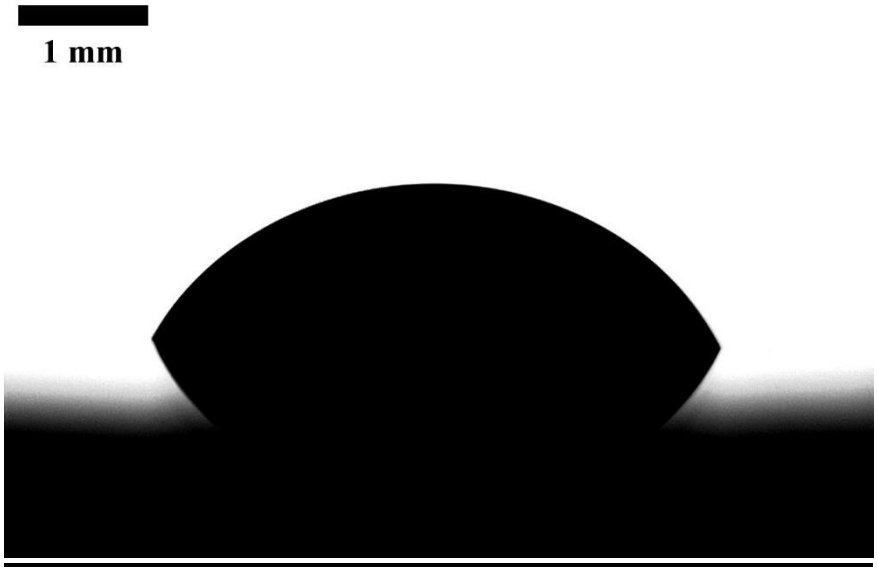

Fig 3.4: TiO_2 – Water nanofluid droplet (Φ=0.1).
left angle = 59.820, right angle = 60.680

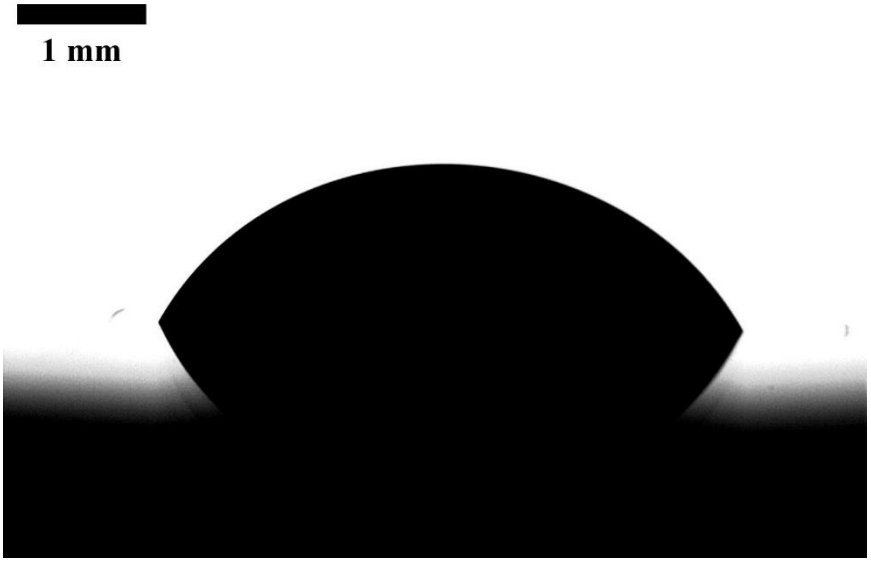

Fig 3.5: TiO_2 – Water nanofluid droplet (Φ = 0.5).
left angle = 58.970, right angle = 59.820

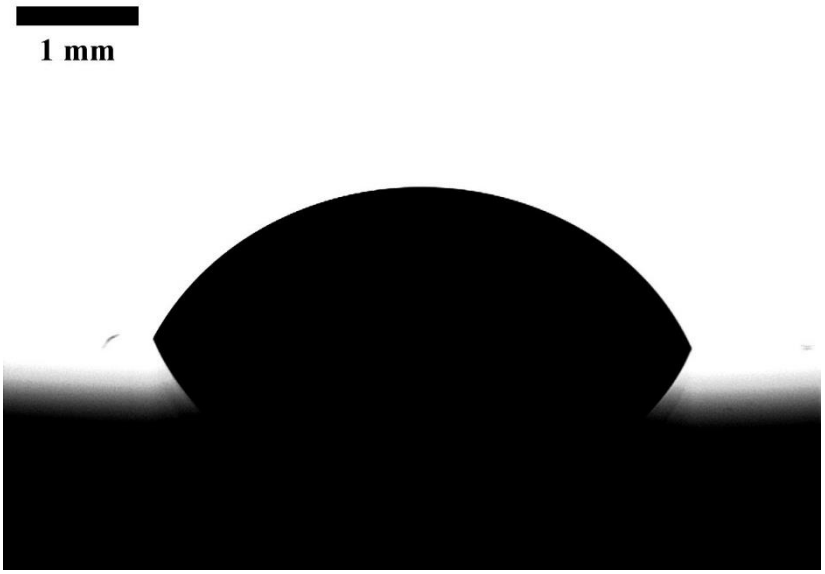

Fig 3.6: TiO_2 – Water nanofluid droplet (Φ = 1.0).
left angle = 60.680, right angle = 61.200

3.1.3 Intensity Graph Analysis:

Gray Intensity Graphs were plotted after the evaporation of the droplet. It was measured as it was shown in the below figures (Fig. 7). One line was drawn in the middle as 0^0 and then rotated anticlockwise for 45^0, 90^0, 135^0. From the plot two axes were generated, where X axis was Distance in pixel and Y axis was Gray Value. For different volume fractions different peaks values were observed.

- **For TiO_2 – Water, Φ = 0.1%:**

Analysing the graph plot for Φ = 0.1%, it was observed that there were two major peaks at periphery as the particle concentration was high there and the coffee ring was formed there. For the line at 0 degree with the origin (Fig. 8) The Left Peak Pixelated Value was 300-450, Average Gray Value was 210 and The Right Peak Pixelated Value was 1950-2080, Average Gray Value was 220. For the line at 45 degree with the origin (Fig. 9) The Left Peak Pixelated Value was 400-520, Average Gray Value was 210 and The Right Peak Pixelated Value was 1950-2080, Average Gray Value was 210. For the line at 90 degree with the origin (Fig. 10) The Left Peak Pixelated Value was 400-500, Average Gray Value was 210 and The Right Peak Pixelated Value was 1950-2080, Average Gray Value was 210. For the line at 135 degree with the origin (Fig. 11) The Left Peak Pixelated Value was 350-500, Average Gray Value was 210 and The Right Peak Pixelated Value was 1950-2080, Average Gray Value was 205.

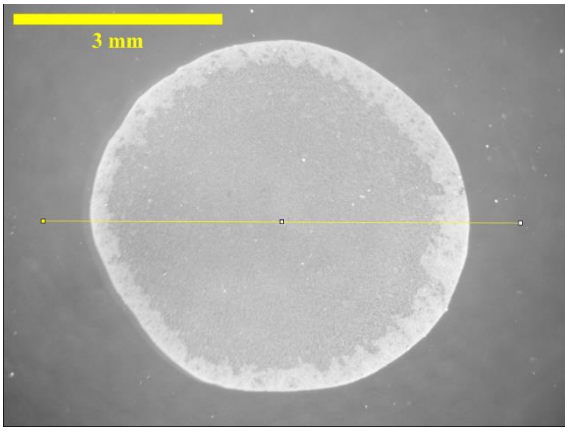

(a) Line angled at 0^0

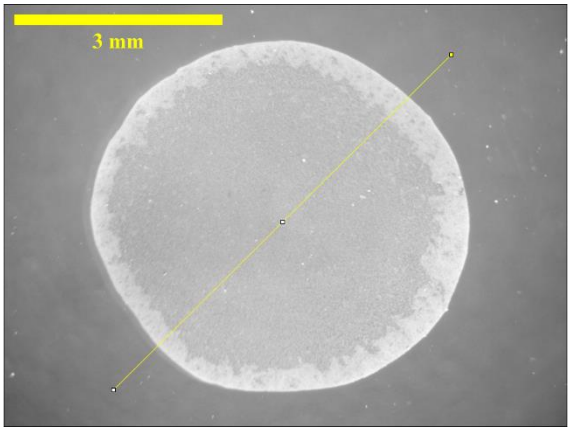

(b) Line angled at 45^0 anticlockwise

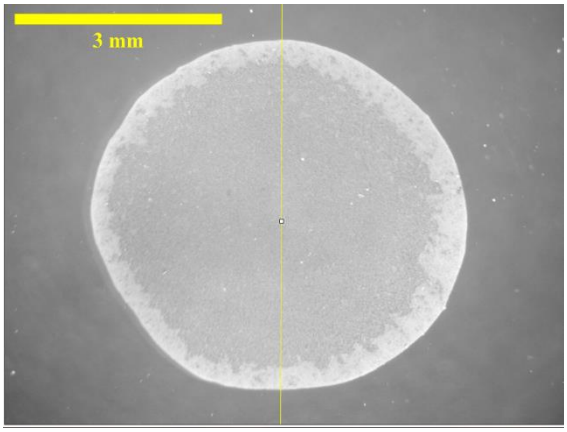

(c) Line angles at 90^0 anticlockwise

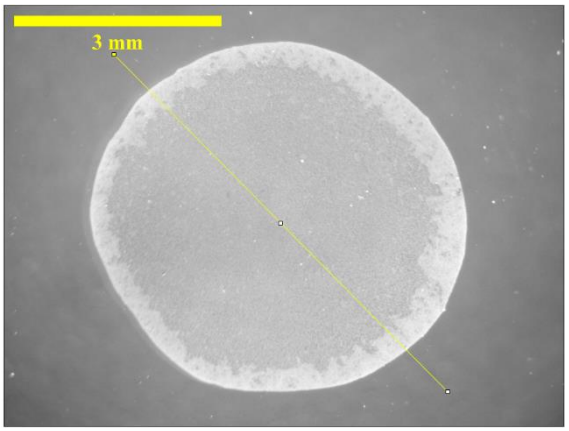

(d) Line angled at 135^0 anticlockwise

Fig 3.7: Image Analysis

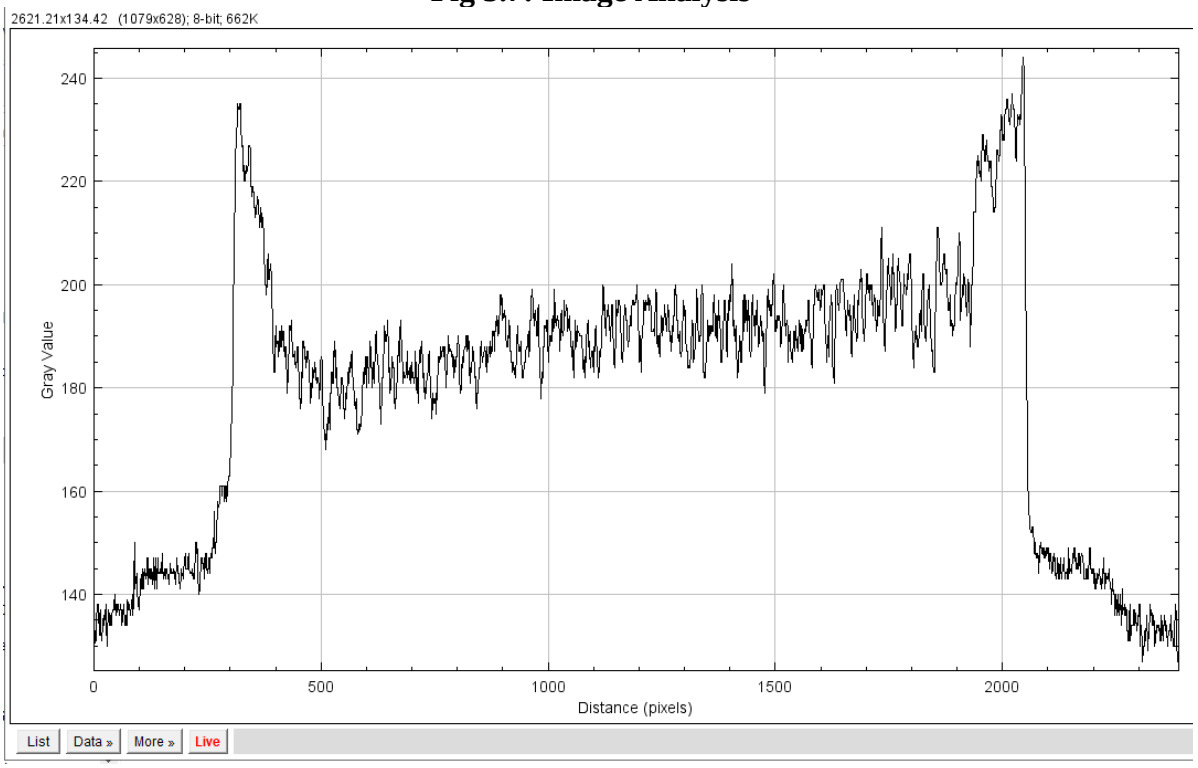

Fig 3.8: Gray Intensity Graph at 0 degree for TiO_2 – Water, Φ = 0.1

Peak Left: Pixel: 300-450, Avg. Gray Value: 210
Peak Right: Pixel: 1950-2080, Avg. Gray Value: 220

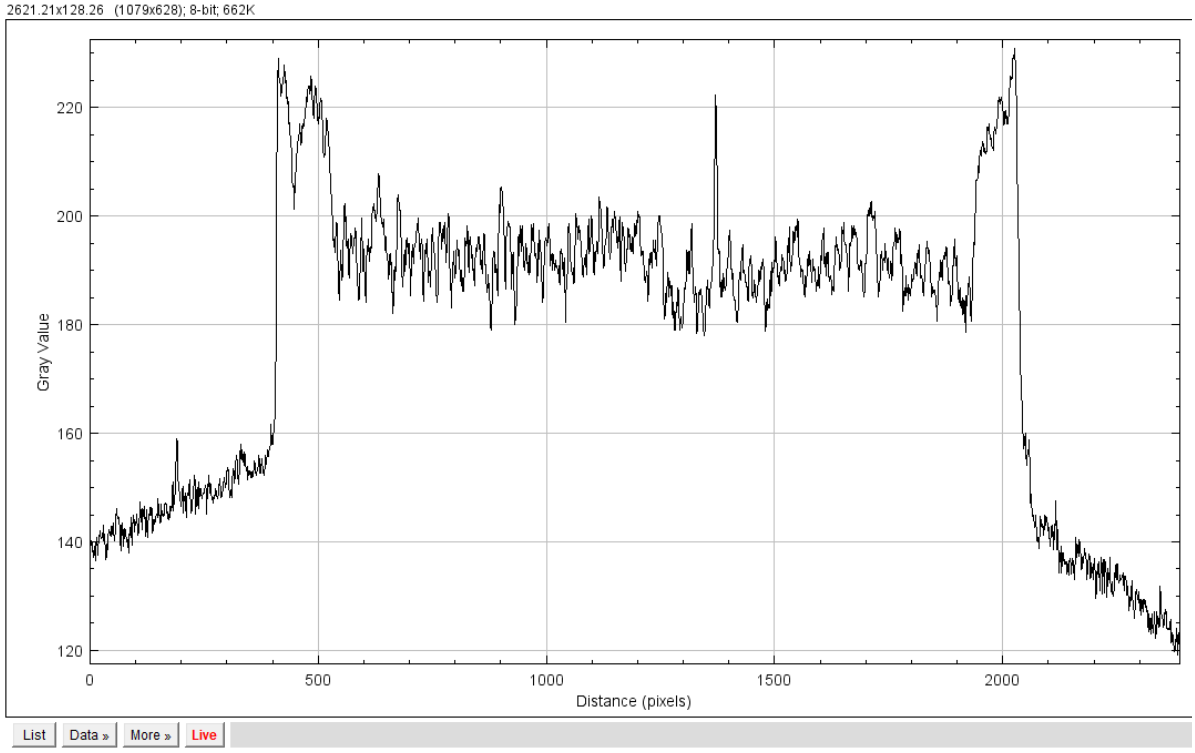

Fig 3.9: Gray Intensity Graph at 45 degree for TiO_2 – Water, Φ = 0.1
Peak Left: Pixel: 400-520, Avg. Gray Value: 210 Peak Right: Pixel: 1950-2080, Avg. Gray Value: 210

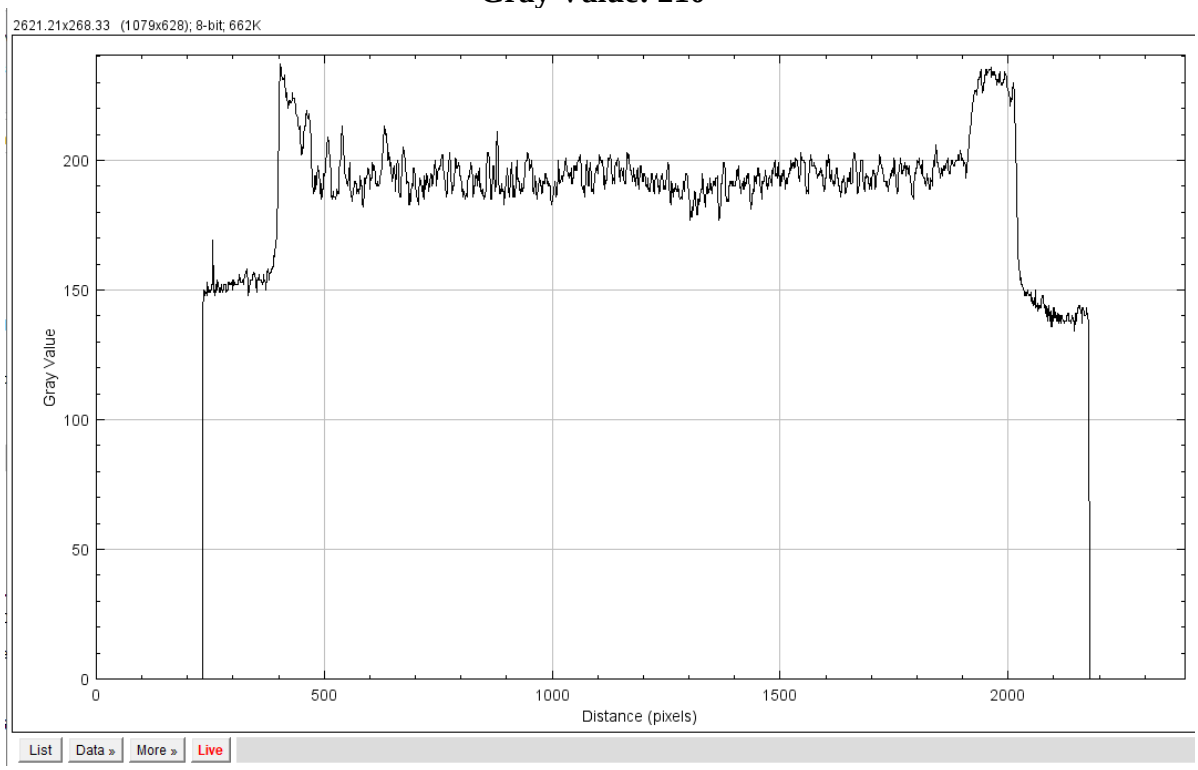

Fig 3.10: Gray Intensity Graph at 90 degree for TiO_2 – Water, Φ = 0.1
Peak Left: Pixel: 400-500, Avg. Gray Value: 210
Peak Right: Pixel: 1950-2080, Avg. Gray Value: 210

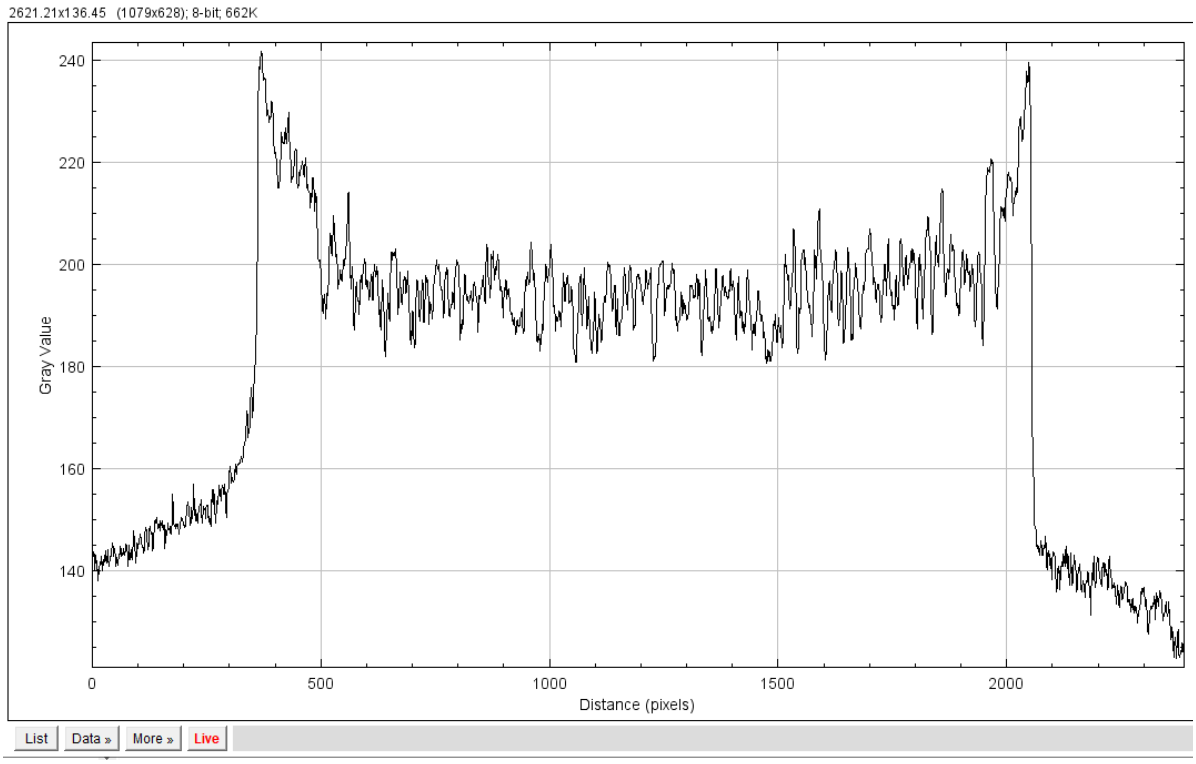

Fig 3.11: Gray Intensity Graph at 135 degree for TiO_2 – Water, Φ = 0.1
Peak Left: Pixel: 350-500, Avg. Gray Value: 210
Peak Right: Pixel: 1950-2080, Avg. Gray Value: 205

- **For TiO_2 – Water, Φ = 0.5%:**

Analysing the graph plot for Φ = 0.5%, it was observed that there were two major peaks at periphery as the particle concentration was high there, as well as slight peak in the middle due to some particle concentration in the middle. For the line at 0 degree with the origin (Fig. 12) The Left Peak Pixelated Distance was 0.22-0.33 mm, Average Gray Value was 190 and The Right Peak Pixelated Distance was 1.65-1.73 mm, Average Gray Value was 181. For the line at 45 degree with the origin (Fig. 13) The Left Peak Pixelated Distance was 0.22-0.33 mm, Average Gray Value was 195 and The Right Peak Pixelated Distance was 1.65-1.73 mm, Average Gray Value was 195. For the line at 90 degree with the origin (Fig. 14) The Left Peak Pixelated Distance was 0.22-0.33 mm, Average Gray Value was 195 and The Right Peak Pixelated Distance was 1.65-1.73 mm, Average Gray Value was 190. For the line at 135 degree with the origin (Fig. 15) The Left Peak Pixelated Distance was 0.22-0.33 mm, Average Gray Value was 190 and The Right Peak Pixelated Distance was 1.65-1.73 mm, Average Gray Value was 181.

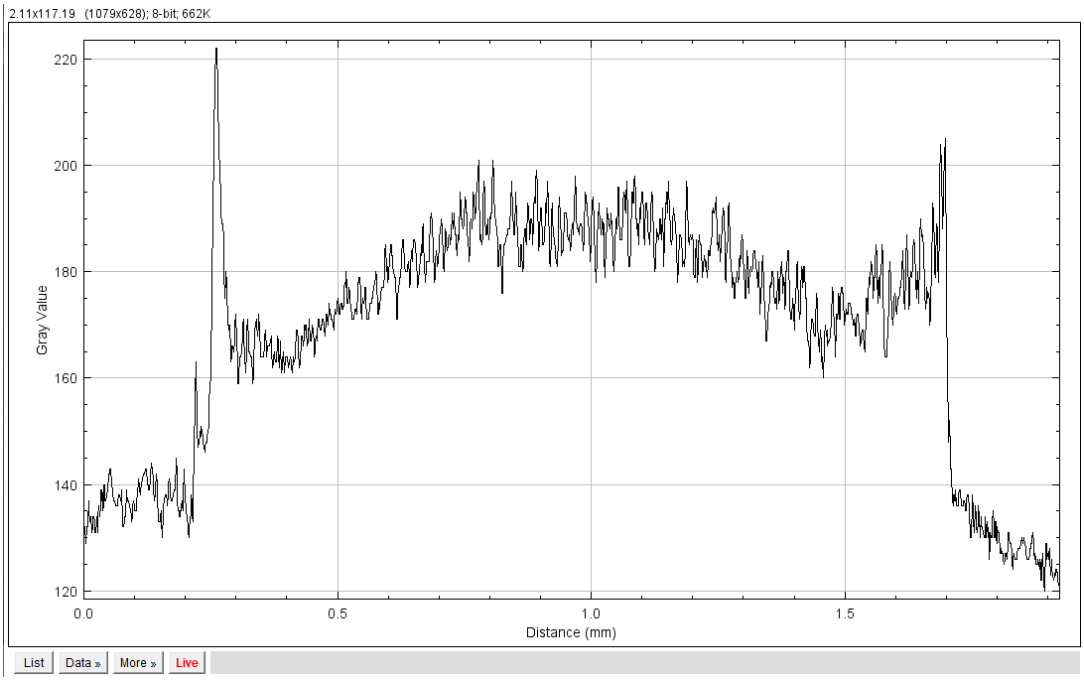

Fig 3.12: Gray Intensity Graph at 0 degree for TiO_2 – Water, Φ = 0.5
Peak Left: Distance: 0.22-0.33 mm, Avg. Gray Value: 190
Peak Right: Distance: 1.65-1.73, Avg. Gray Value: 181

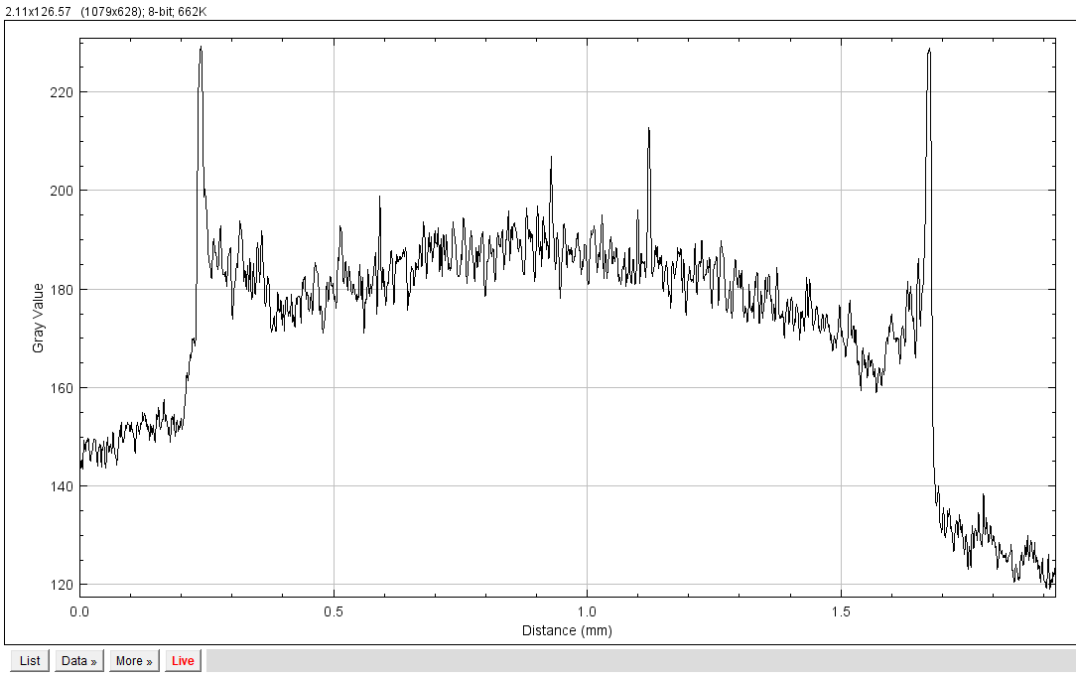

Fig 3.13: Gray Intensity Graph at 45 degree for TiO_2 – Water, Φ = 0.5
Peak Left: Distance: 0.22-0.33 mm, Avg. Gray Value: 195
Peak Right: Distance: 1.65-1.73, Avg. Gray Value: 195

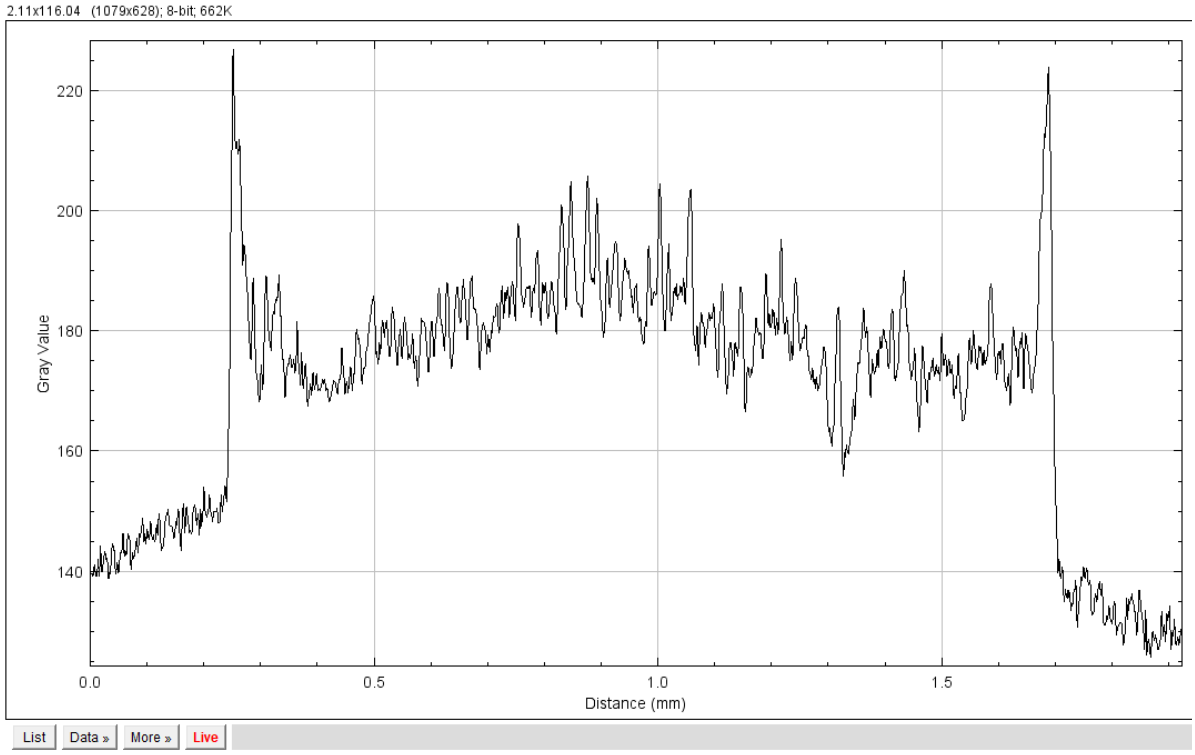

Fig 3.14: Gray Intensity Graph at 90 degree for TiO_2 – Water, Φ = 0.5
Peak Left: Distance: 0.22-0.33 mm, Avg. Gray Value: 195
Peak Right: Distance: 1.65-1.73, Avg. Gray Value: 190

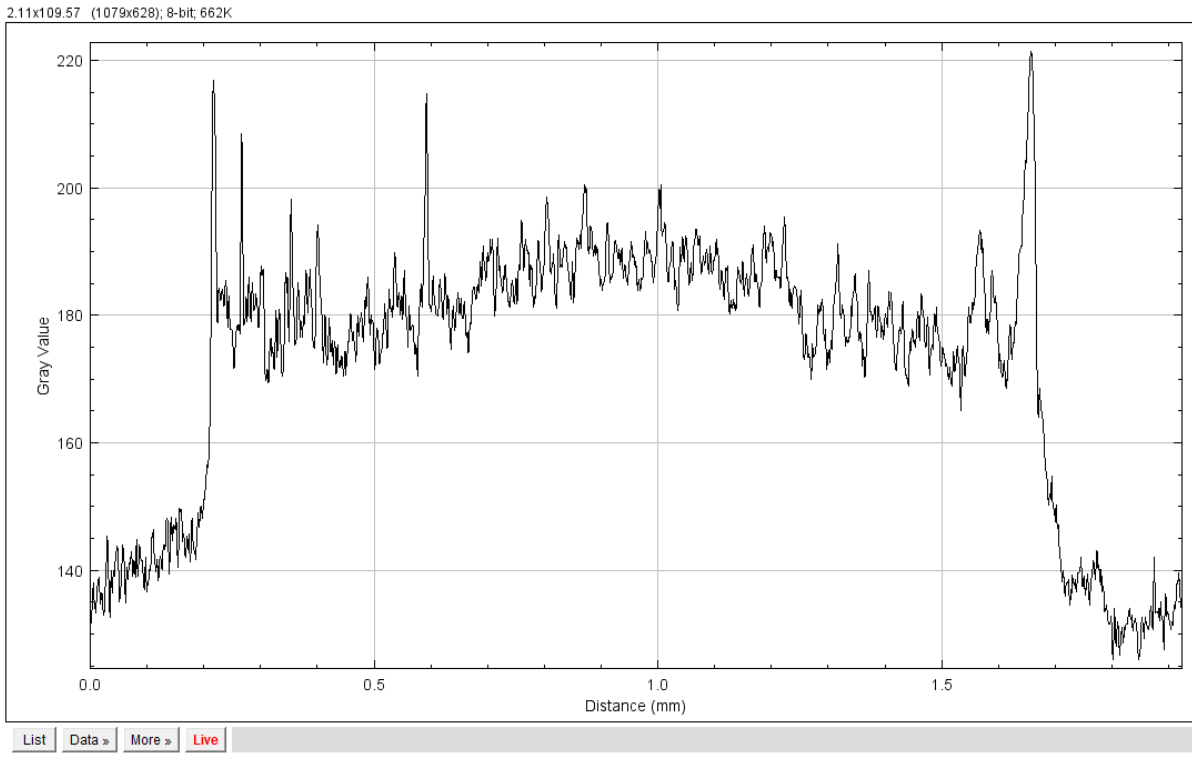

Fig 3.15: Gray Intensity Graph at 135 degree for TiO_2 – Water, Φ = 0.5
Peak Left: Distance: 0.22-0.33 mm, Avg. Gray Value: 190
Peak Right: Distance: 1.65-1.73, Avg. Gray Value: 181

- **For TiO_2 – Water, Φ = 1.0%:**

Analysing the graph plot for Φ = 1.0%, it was observed that there were many peaks along the line means the particles were distributed uniformly along the all area of the pattern. For the line at 0 degree with the origin (Fig. 16) Average Gray Value was 183. For the line at 45 degree with the origin (Fig. 17) Average Gray Value was 185. For the line at 90 degree with the origin (Fig. 18) Average Gray Value was 187. For the line at 135 degree with the origin (Fig. 19) Average Gray Value was 185.

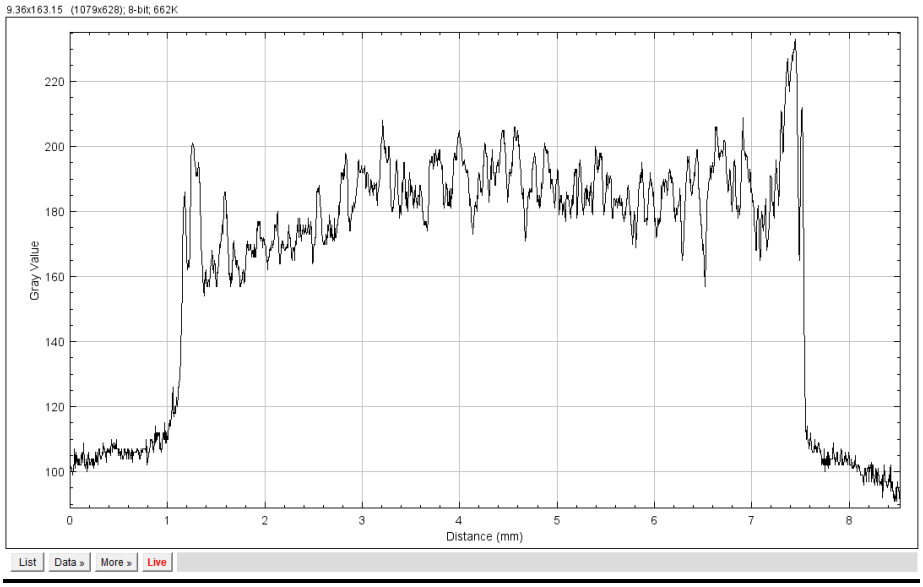

Fig 3.16: Gray Intensity Graph at 0 degree for TiO_2 – Water, Φ = 1.0
Avg. Gray Value: 183

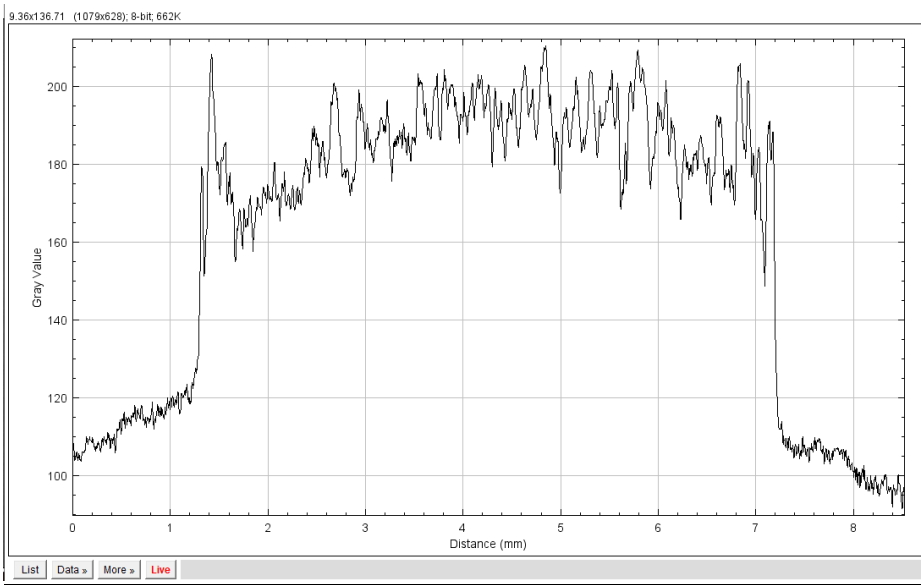

Fig 3.17: Gray Intensity Graph at 45 degree for TiO_2 – Water, Φ = 1.0
Avg. Gray Value: 185

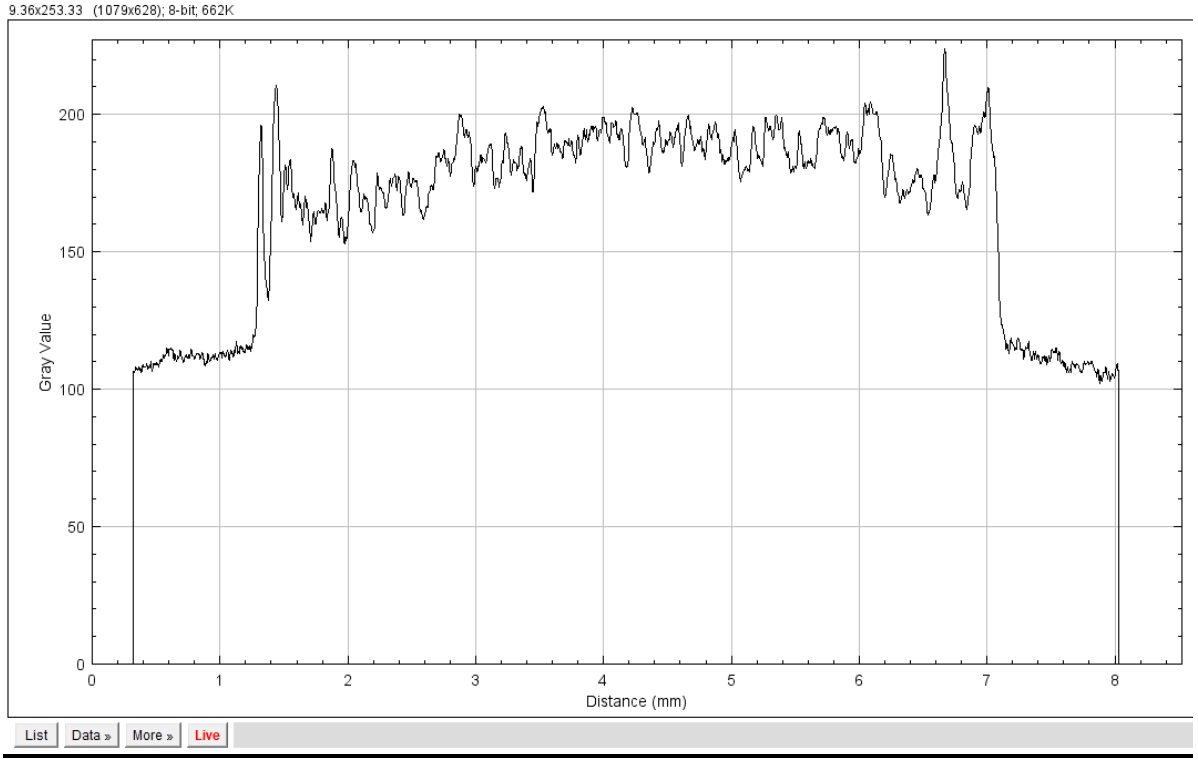

Fig 3.18: Gray Intensity Graph at 90 degree for TiO_2 – Water, Φ = 1.0
Avg. Gray Value: 187

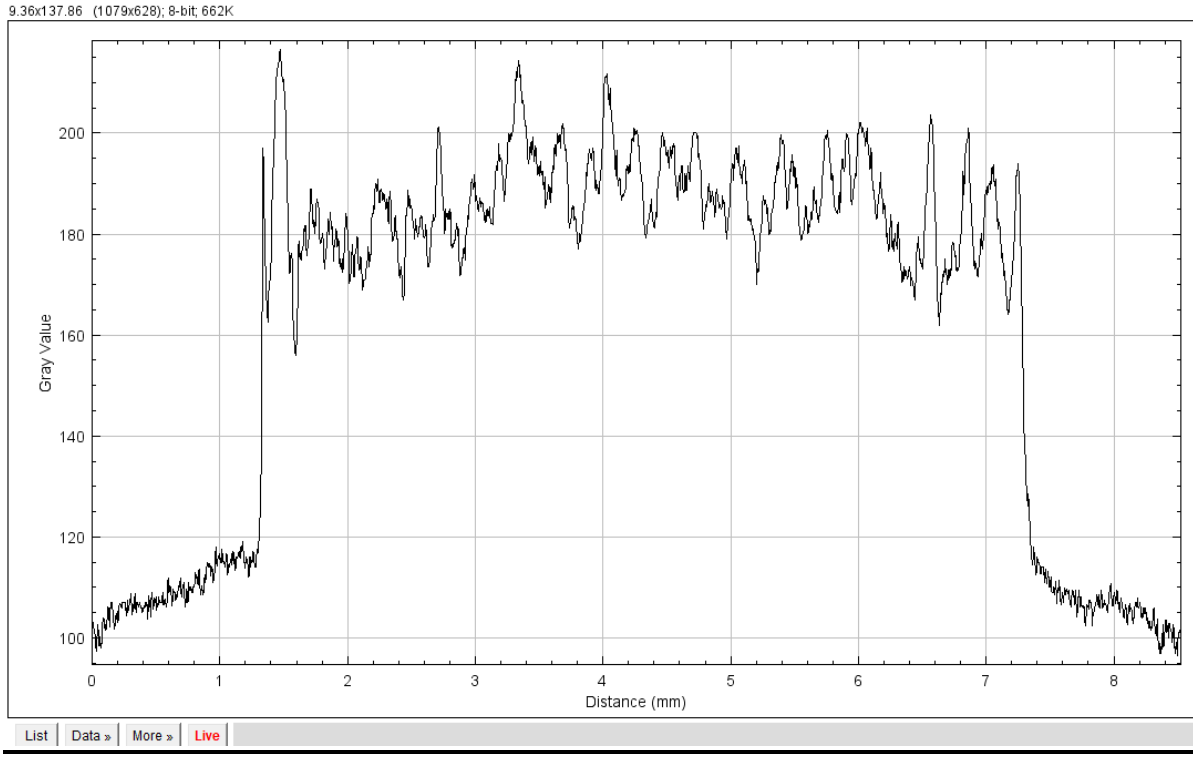

Fig 3.19: Gray Intensity Graph at 135 degree for TiO_2 – Water, Φ = 1.0
Avg. Gray Value: 185

3.2 Nanofluid With Surfactant:

3.2.1 TiO_2-Water with CTAB (Φ = 0.5% & Φ = 1.0%):

a) Pattern Analysis:

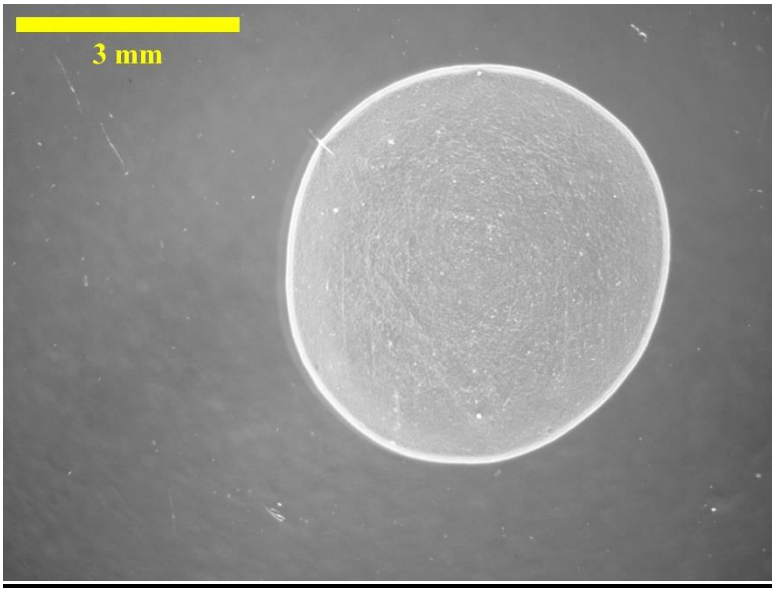

Fig 3.20: TiO_2 – Water CTAB Nanofluid after evaporation droplet pattern (Φ=0.5%) deposited on Glass Substrate. Surfactant: Nano Particle = 1:10. Volume ~9.23 µL. Droplet Pattern Width: ~5.158 mm, Height: ~5.376 mm. Generated Ring varies from ~0.1 mm to ~0.12 mm in thickness

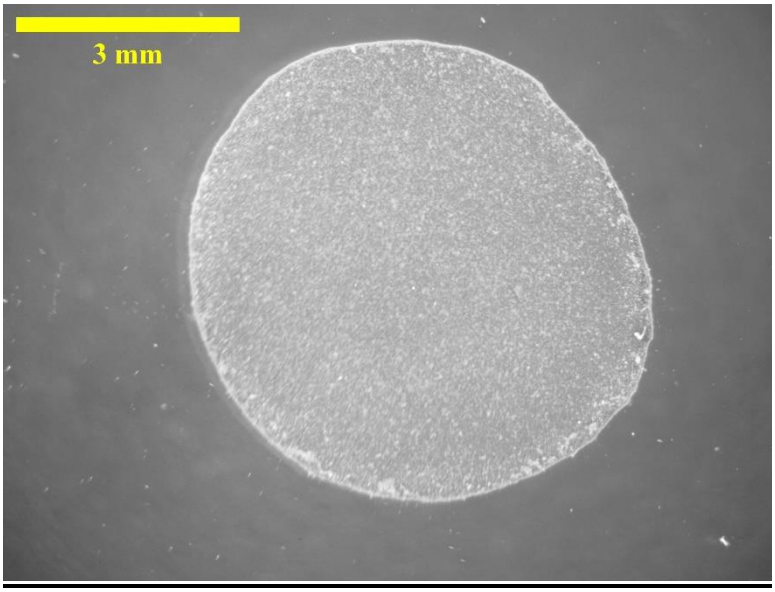

Fig 3.21: TiO_2 – Water CTAB Nanofluid after evaporation droplet pattern (Φ=1.0%) deposited on Glass Substrate. Surfactant: Nano Particle = 1:10. Volume ~9.23 µL. Droplet Pattern Width: ~6.202 mm, Height: ~6.222 mm. Generated Ring varies from ~0.02 mm to ~0.06 mm in thickness

For TiO_2-Water with CTAB (Φ=0.5%), (Fig. 20) a perfect coffee ring was found. Where the height was measured as ~5.376 mm and width was measured as ~5.158 mm and the thickness

was measured as from ~0.1 mm to ~0.12 mm. whereas for (Φ=1.0%) (Fig. 21) a very thin ring was generated, where the pattern height was measured as ~6.222 mm and width as ~6.202 mm. ring thickness was ~0.02 mm to ~0.06 mm.

b) Contact Angle Analysis:

Analysing the results of the Contact angles for TiO_2-Water with CTAB for Φ=0.5% and Φ=1.0%, there was 3 – 4 degree of difference in right angle and left contact angles in Φ=0.5% and Φ=1.0%, for Φ=0.5% (Fig. 22) left angle measured as 61.54^0 and right angle measured as 62.4^0. Similarly, for Φ=1.0% (Fig. 23) left angle measured as 63.26^0 and right angle measured as 65.84^0.

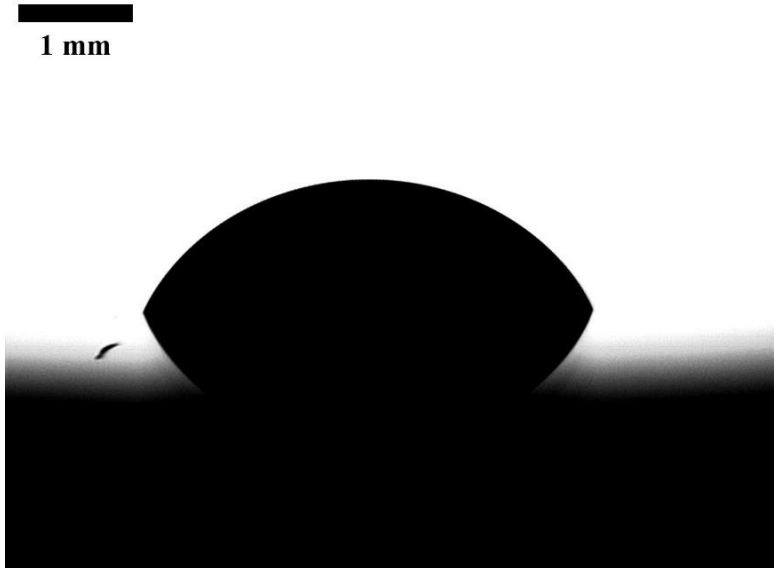

Fig 3.22: TiO_2 – Water CTAB nanofluid droplet (Φ = 0.5). left angle = 61.540, right angle = 62.40

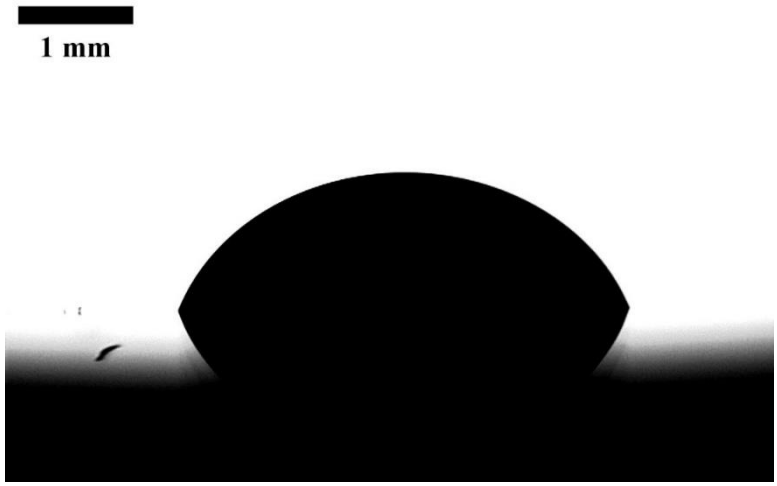

Fig 3.23: TiO_2 – Water CTAB nanofluid droplet (Φ = 1.0).

left angle = 63.260, right angle = 65.840

c) Intensity Graph Analysis:

➢ For TiO_2 – Water with CTAB (Φ = 0.5%):

Analysing the graph plot for TiO_2 – Water with CTAB (Φ = 0.5%), it is observed that there were two major peaks at periphery as the particle concentration was high there. For the line at 0 degree with the origin (Fig. 24) The Left Peak Pixelated Distance was 1.0-1.2 mm, Average Gray Value was 220 and The Right Peak Pixelated Distance was 6.0-6.2 mm, Average Gray Value was 215. For the line at 45 degree with the origin (Fig. 25) The Left Peak Pixelated Distance was 0.8-1.0 mm, Average Gray Value was 220 and The Right Peak Pixelated Distance was 5.8-6.1 mm, Average Gray Value was 210. For the line at 90 degree with the origin (Fig. 26) The Left Peak Pixelated Distance was 0.7-0.98 mm, Average Gray Value was 215 and The Right Peak Pixelated Distance was 6.0-6.2 mm, Average Gray Value was 215. For the line at 135 degree with the origin (Fig. 27) The Left Peak Pixelated Distance was 0.6-0.8 mm, Average Gray Value was 210 and The Right Peak Pixelated Distance was 5.9-6.1 mm, Average Gray Value was 220.

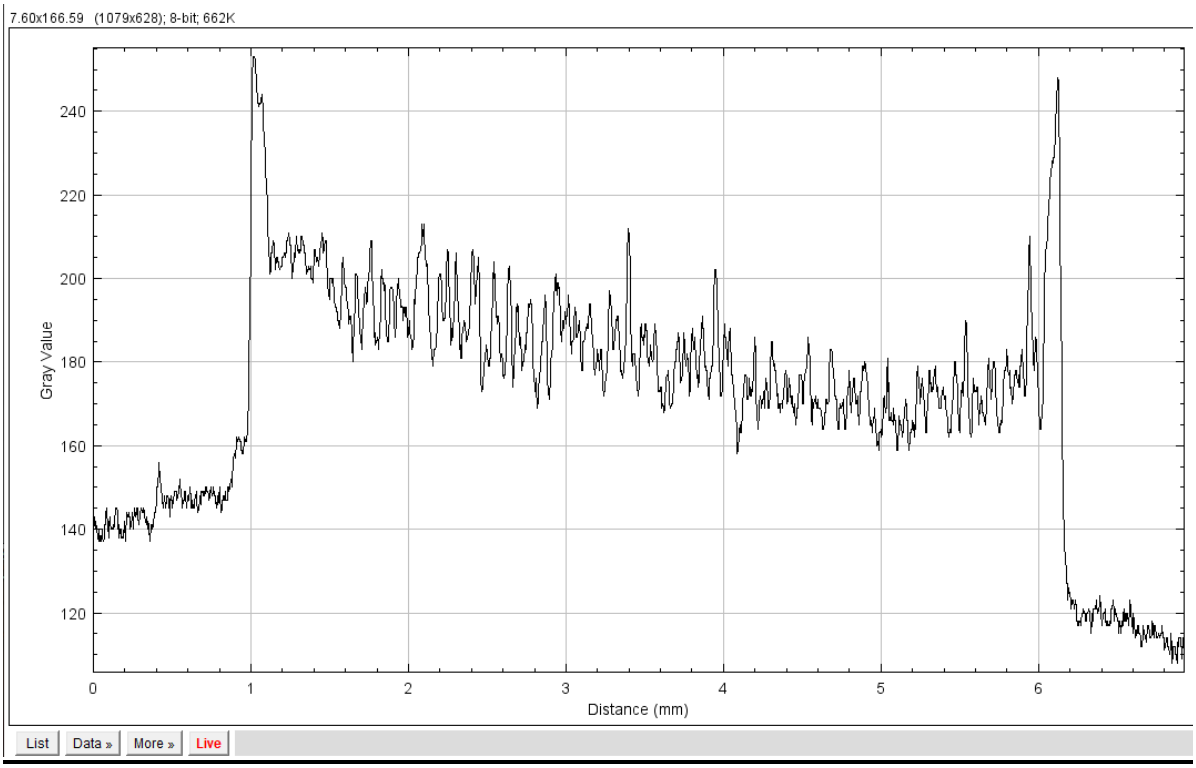

Fig 3.24: Gray Intensity Graph at 0 degree for TiO_2 – Water CTAB, Φ = 0.5
Peak Left: Distance: 1.0-1.2 mm, Avg. Gray Value: 220
Peak Right: Distance: 6.0-6.2 mm, Avg. Gray Value: 215

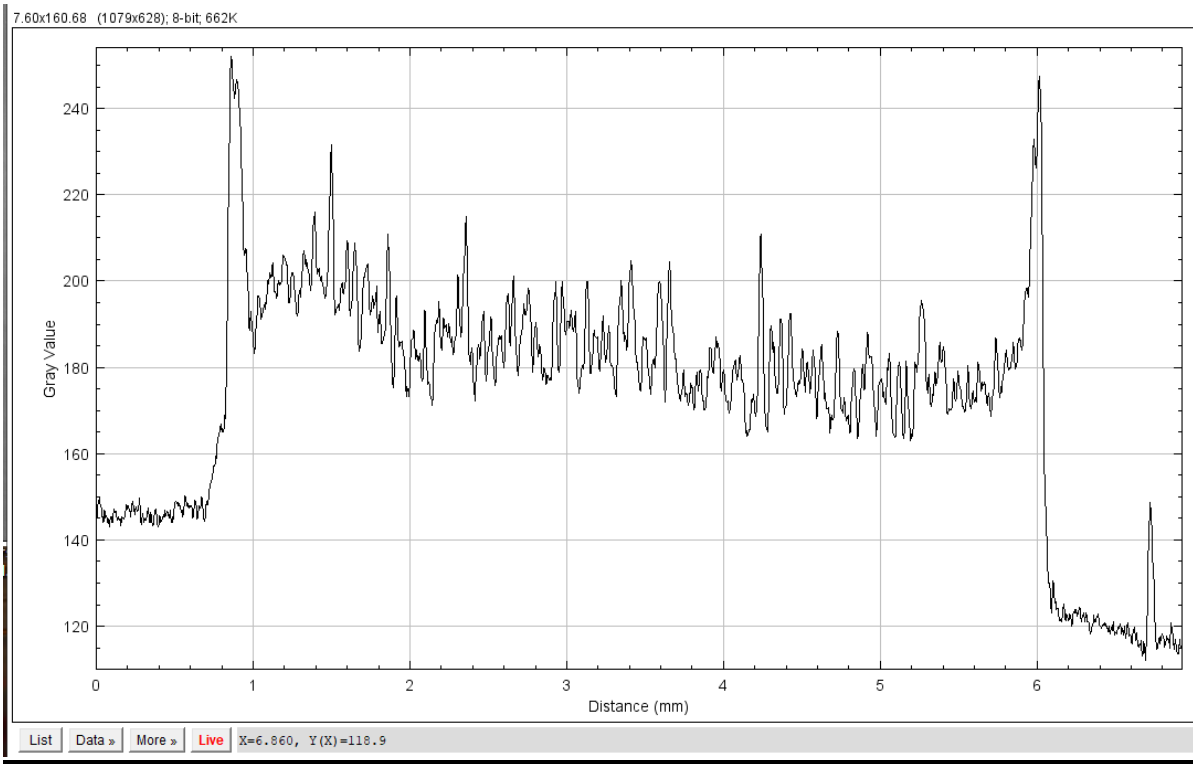

Fig 3.25: Gray Intensity Graph at 45 degree for TiO_2 – Water CTAB, Φ = 0.5
Peak Left: Distance: 0.8-1.0 mm, Avg. Gray Value: 220
Peak Right: Distance: 5.8-6.1 mm, Avg. Gray Value: 210

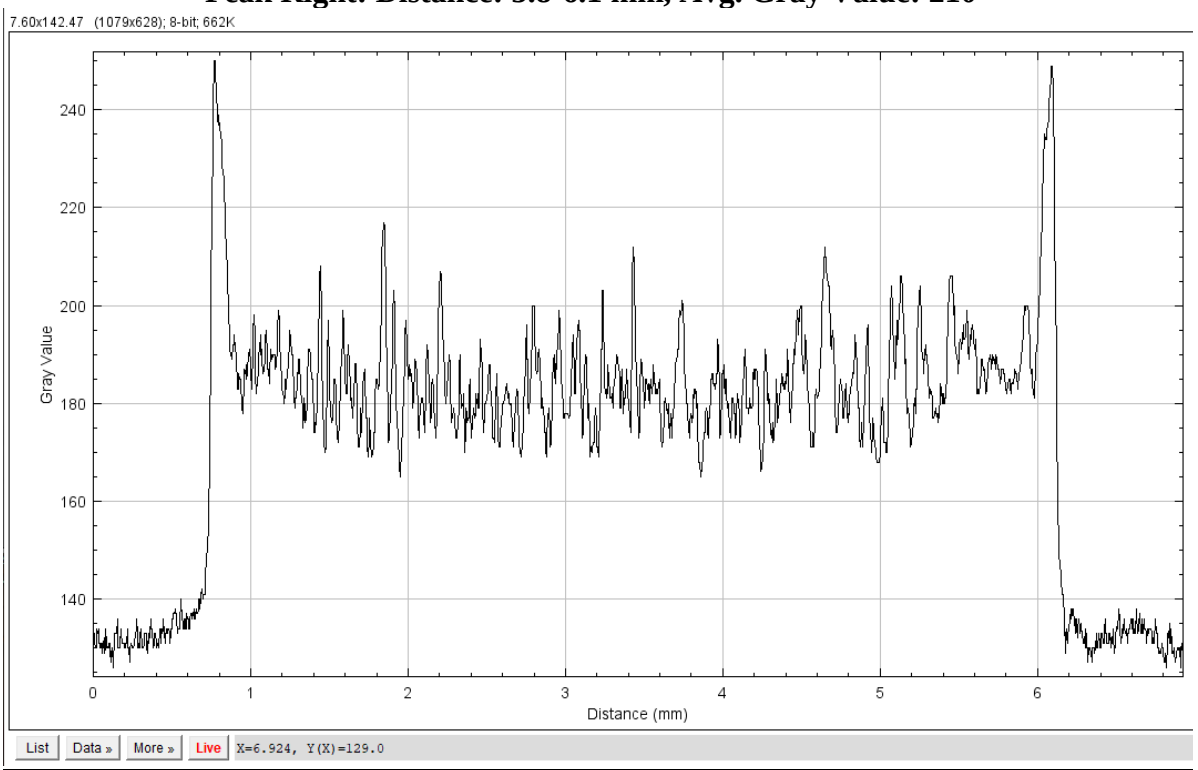

Fig 3.26: Gray Intensity Graph at 90 degree for TiO_2 – Water CTAB, Φ = 0.5
Peak Left: Distance: 0.7-0.98 mm, Avg. Gray Value: 215
Peak Right: Distance: 6.0-6.2 mm, Avg. Gray Value: 215

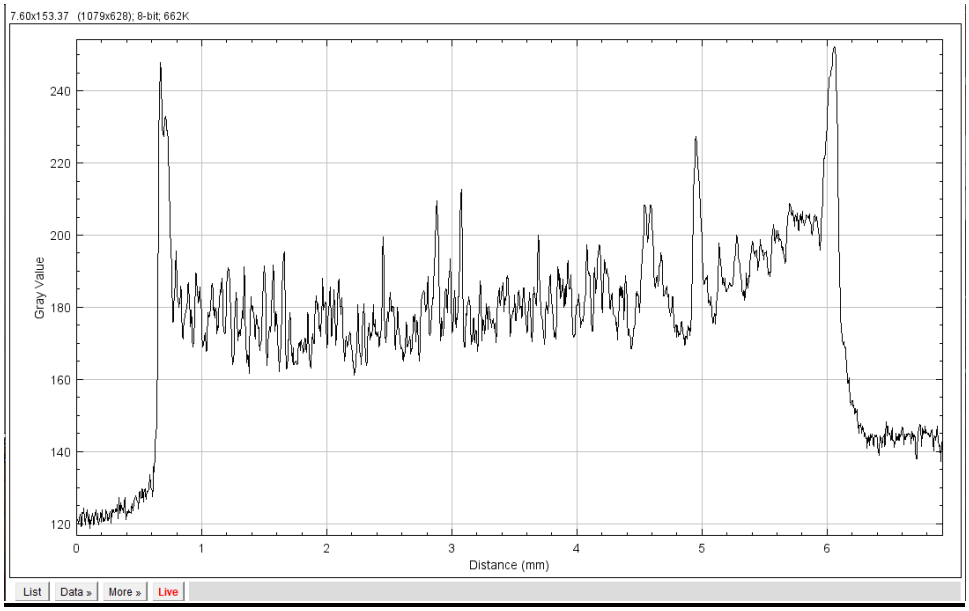

Fig 3.27: Gray Intensity Graph at 135 degree for TiO_2 – Water CTAB, Φ = 0.5
Peak Left: Distance: 0.6-0.8 mm, Avg. Gray Value: 210
Peak Right: Distance: 5.9-6.1 mm, Avg. Gray Value: 220

- **For TiO_2 – Water with CTAB (Φ = 1.0%):**

Analysing the graph plot for TiO_2 – Water with CTAB (Φ = 1.0%), it is observed that there were many peaks along the line means the particles were distributed uniformly along the all area of the pattern. For the line at 0 degree with the origin (Fig. 28) Average Gray Value was 185. For the line at 45 degree with the origin (Fig. 29) Average Gray Value was 185. For the line at 90 degree with the origin (Fig. 30) Average Gray Value was 185. For the line at 135 degree with the origin (Fig. 31) Average Gray Value was 182.

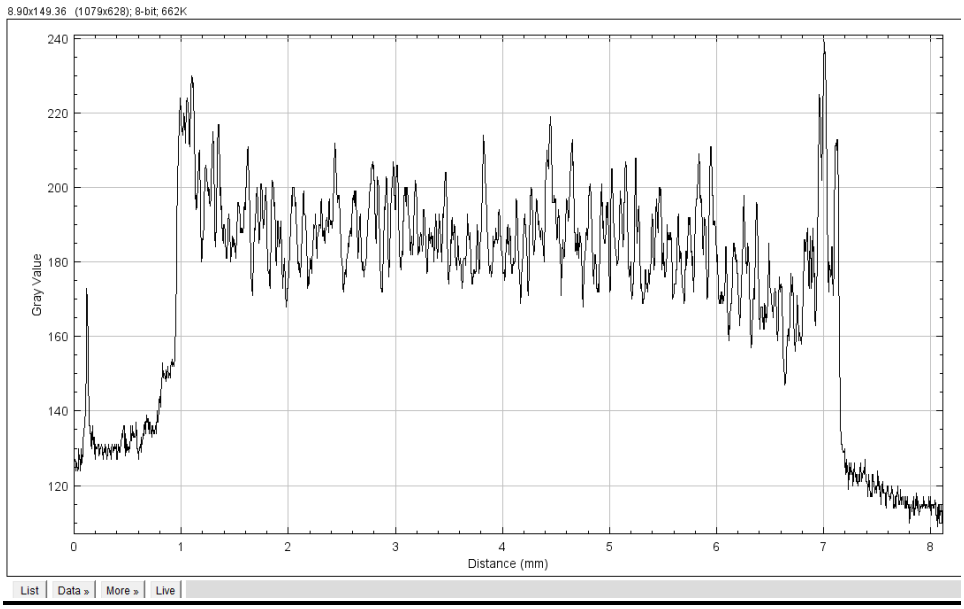

Fig 3.28: Gray Intensity Graph at 0 degree for TiO_2 – Water CTAB, Φ = 1.0

Mid-Range Avg. Gray Value: 185

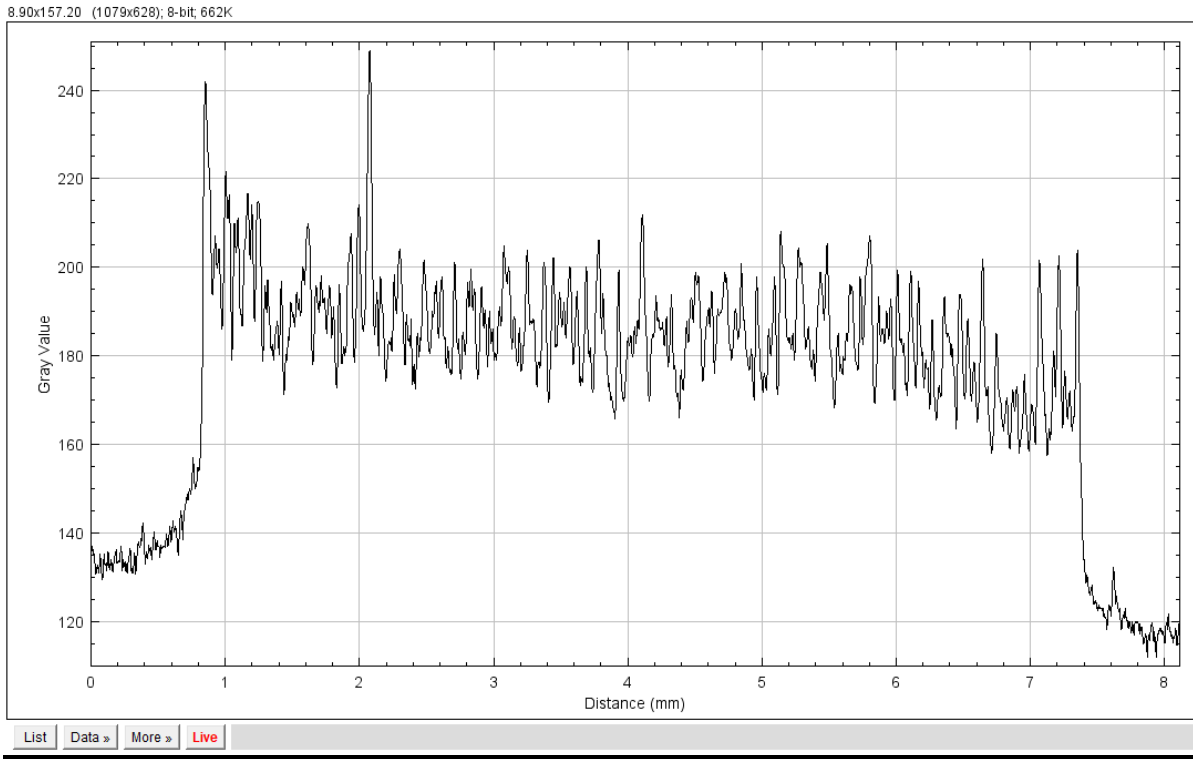

Fig 3.29: Gray Intensity Graph at 45 degree for TiO_2 – Water CTAB, Φ = 1.0
Mid-Range Avg. Gray Value: 185

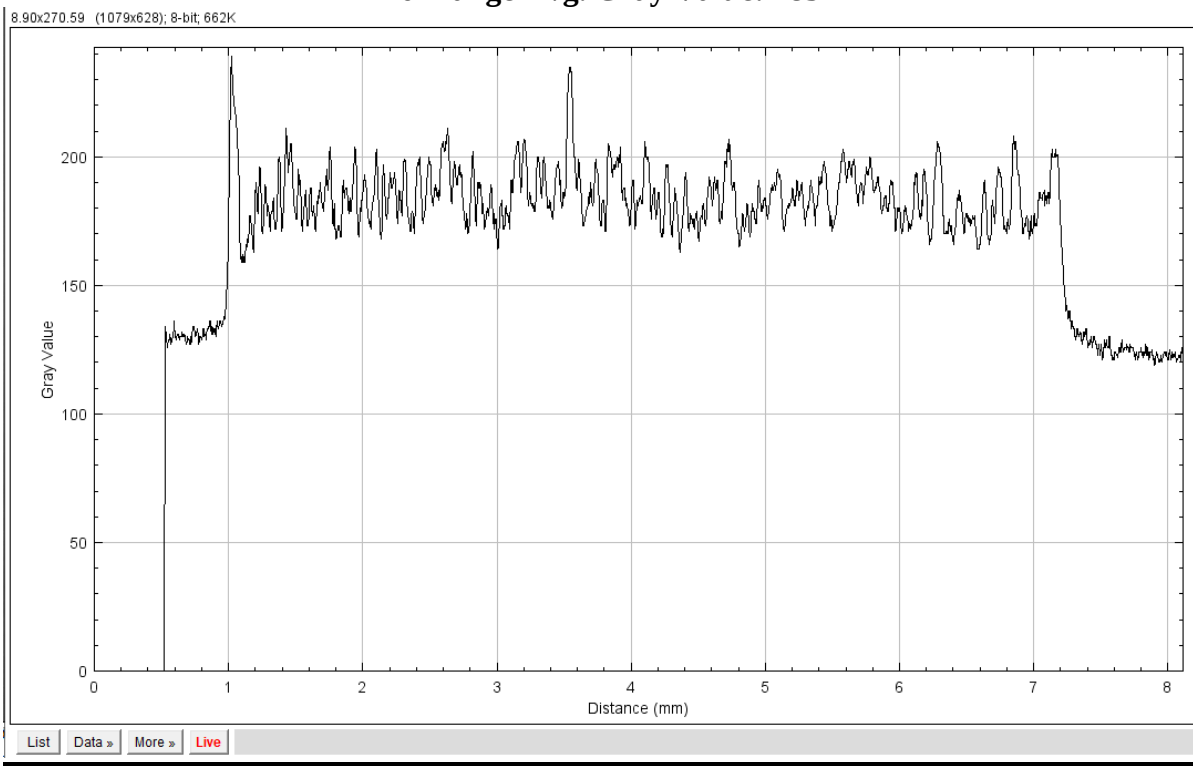

Fig 3.30: Gray Intensity Graph at 90 degree for TiO_2 – Water CTAB, Φ = 1.0
Mid-Range Avg. Gray Value: 185

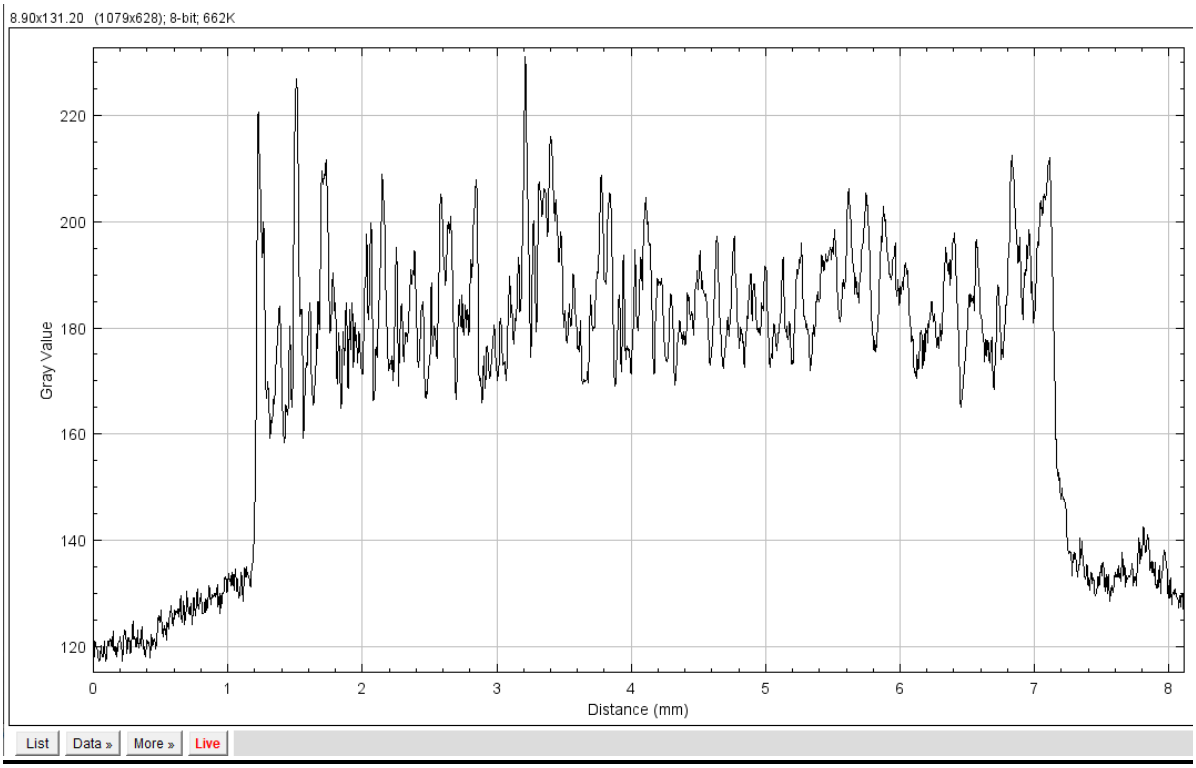

Fig 3.31: Gray Intensity Graph at 135 degree for TiO_2 – Water CTAB, Φ = 1.0
Mid-Range Avg. Gray Value: 182

3.2.2 TiO_2-Water with AA (Φ = 0.5% & Φ = 1.0%):

a) Pattern Analysis:

For TiO_2-Water with Acetic Acid (AA) (Φ=0.5%), (Fig. 32) an interesting pattern was noticed. The pattern looks like a flower. Even though the proper reason was unknown still there was a chance that change was humidity or temperature may have affected it. Also, acetic acid has strong hydrogen bonds which may have caused such beautiful structure to form. The height of the pattern was measured as ~1.041 mm and width was measured as ~1.031 mm. Whereas for (Φ=1.0%) (Fig. 33) again uniform pattern was observed, where the pattern height was measured as ~4.774 mm and width as ~4.56 mm.

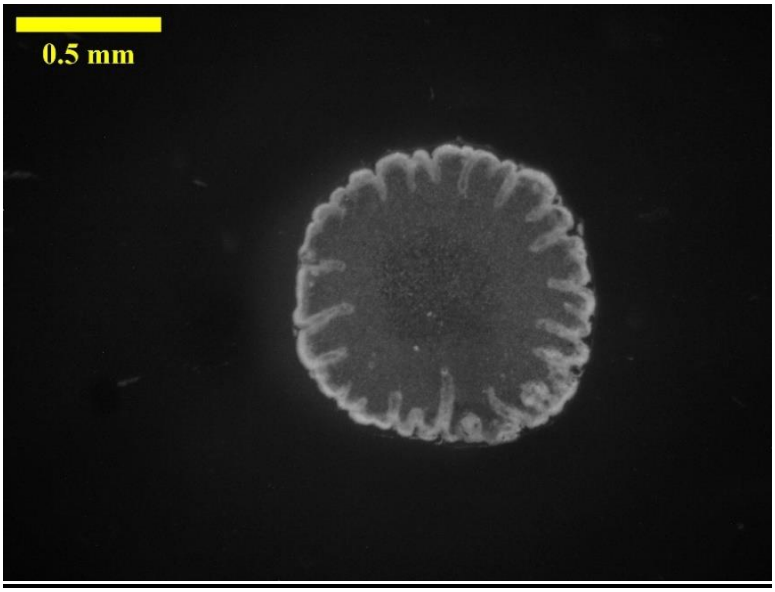

Fig 3.32: TiO_2 – Water AA Nanofluid after evaporation droplet pattern (Φ=0.5%) deposited on Glass Substrate. Volume ~8.17 µL. Droplet Pattern Width: ~1.031 mm, Height: ~1.041 mm.

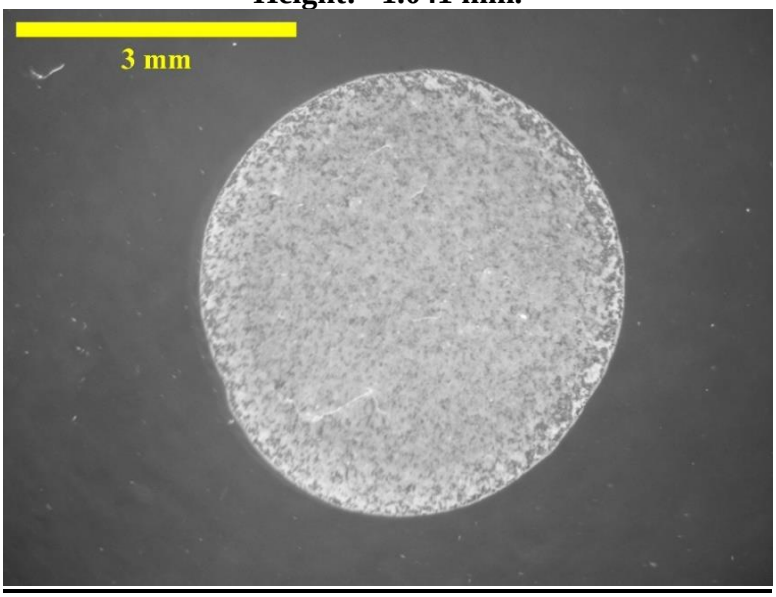

Fig 3.33: TiO_2 – Water AA Nanofluid after evaporation droplet pattern (Φ=1.0%) deposited on Glass Substrate. Volume ~8.17 µL. Droplet Pattern Width: ~4.56 mm, Height: ~4.774 mm.

b) Contact Angle Analysis:

Analysing the results of the Contact angles for TiO_2-Water with Acetic Acid (AA) for Φ=0.5% and Φ=1.0%, there isn't much difference in right angle and left contact angles in Φ=0.5% and Φ=1.0%, for Φ=0.5% (Fig. 34) left angle measured as 62.92^0 and right angle measured as 64.98^0. Similarly, for Φ=1.0% (Fig. 35) left angle measured as 59.82^0 and right angle measured as 60.68^0

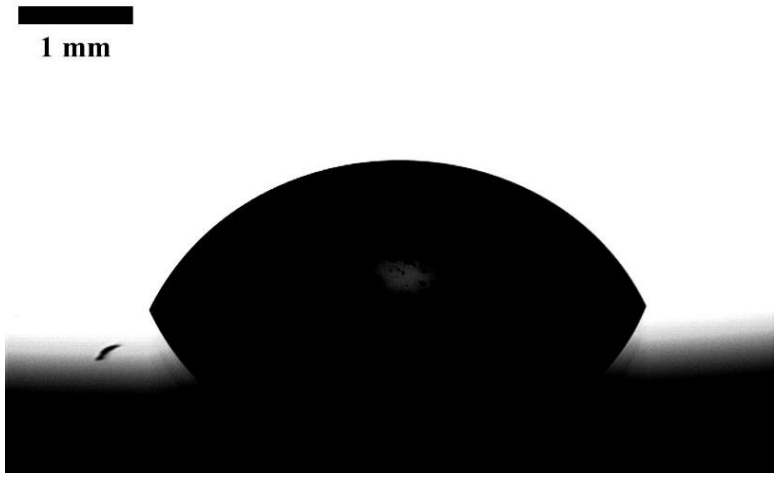

Fig 3.34: TiO_2 – Water AA nanofluid droplet (Φ = 0.5). left angle = 62.920, right angle = 64.980

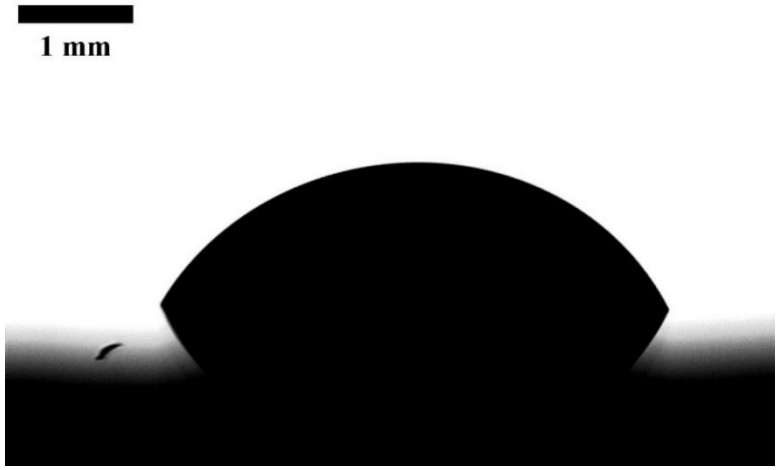

Fig 3.35: TiO_2 – Water nanofluid droplet (Φ = 0.5). left angle = 59.820, right angle = 60.680

c) Intensity Graph Analysis:

- **For TiO_2 – Water with Acetic Acid (AA) (Φ = 0.5%):**

Analysing the graph plot for TiO_2 – Water with Acetic Acid (AA) (Φ = 0.5%), it is found that there were two major peaks at periphery as the particle concentration was high there. For the line at 0 degree with the origin (Fig. 36) The Left Peak Pixelated Distance was 0.16-0.26 mm, Average Gray Value was 110 and The Right Peak Pixelated Distance was 1.15-1.24 mm, Average Gray Value was 110. For the line at 45 degree with the origin (Fig. 37) The Left Peak Pixelated Distance was 0.16-0.22 mm, Average Gray Value was 100 and The Right Peak Pixelated Distance was 1.1-1.26 mm, Average Gray Value was 110. For the line at 90 degree with the origin (Fig. 38) The Left Peak Pixelated Distance was 0.15-0.23 mm, Average Gray

Value was 110 and The Right Peak Pixelated Distance was 1.0-1.18 mm, Average Gray Value was 100. For the line at 135 degree with the origin (Fig. 39) The Left Peak Pixelated Distance was 0.13-0.24 mm, Average Gray Value was 100 and The Right Peak Pixelated Distance was 1.14-1.23 mm, Average Gray Value was 100.

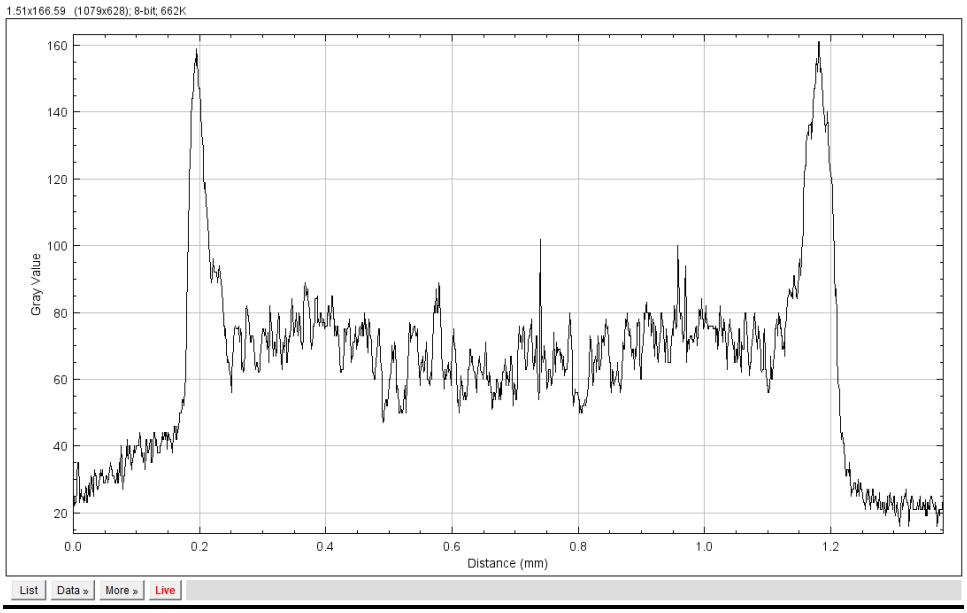

Fig 3.36: Gray Intensity Graph at 0 degree for TiO_2 – Water AA, Φ = 0.5
Peak Left: Distance: 0.16-0.26 mm, Avg. Gray Value: 110
Peak Right: Distance: 1.15-1.24, Avg. Gray Value: 110

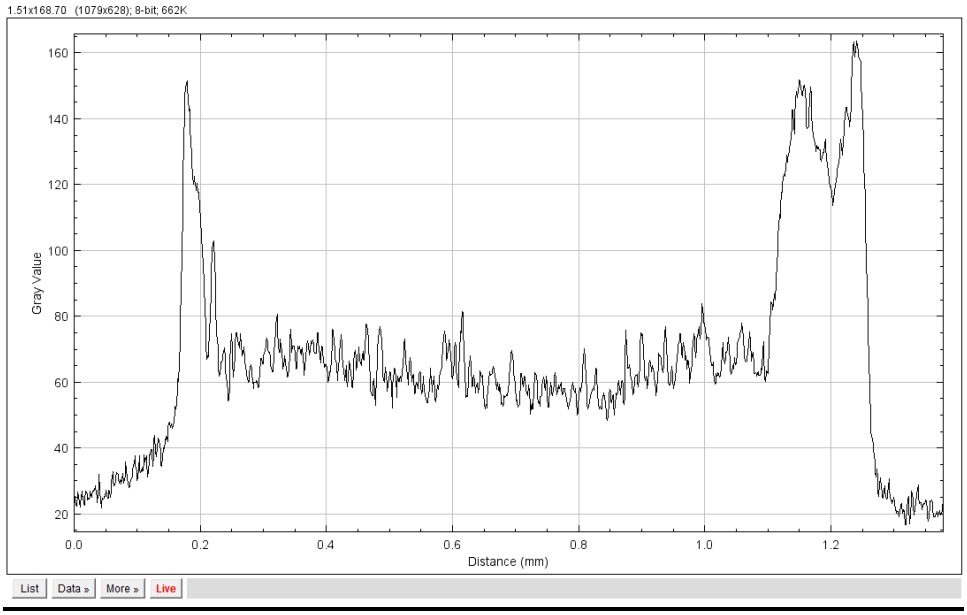

Fig 3.37: Gray Intensity Graph at 45 degree for TiO_2 – Water AA, Φ = 0.5
Peak Left: Distance: 0.16-0.22 mm, Avg. Gray Value: 100
Peak Right: Distance: 1.1-1.26, Avg. Gray Value: 110

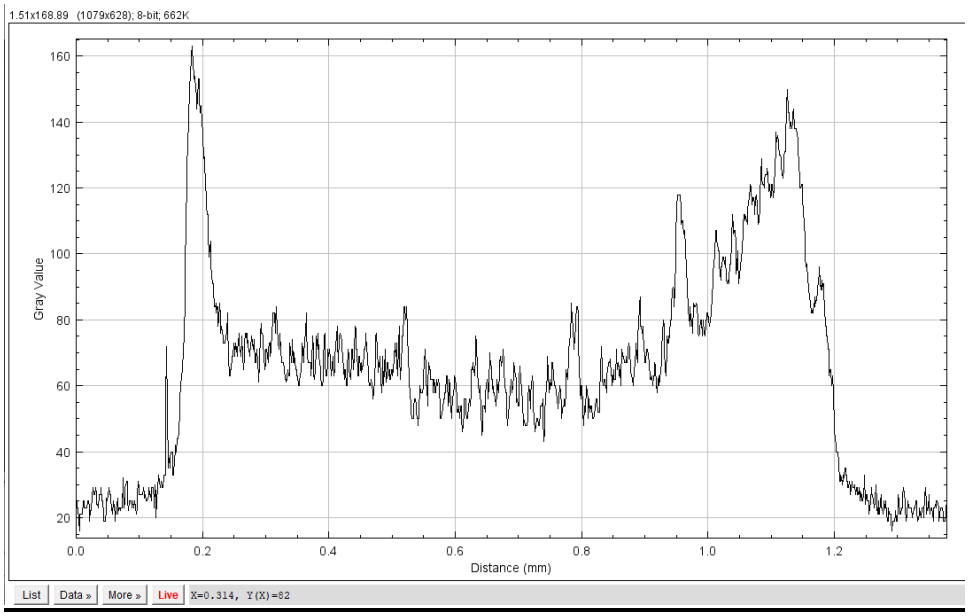

Fig 3.38: Gray Intensity Graph at 90 degree for TiO_2 – Water AA, Φ = 0.5
Peak Left: Distance: 0.15-0.23 mm, Avg. Gray Value: 110
Peak Right: Distance: 1.0-1.18, Avg. Gray Value: 100

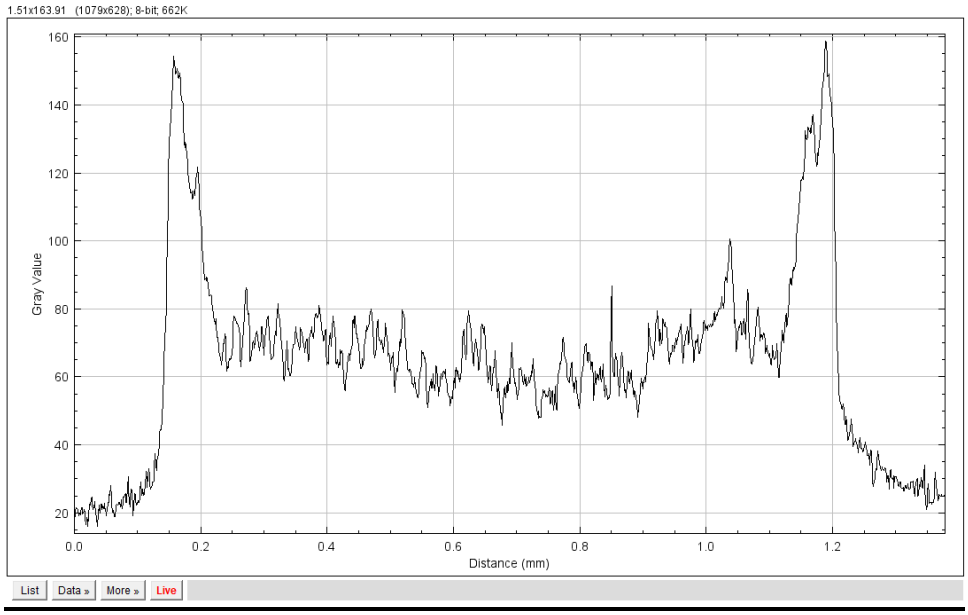

Fig 3.39: Gray Intensity Graph at 135 degree for TiO_2 – Water AA, Φ = 0.5
Peak Left: Distance: 0.13-0.24 mm, Avg. Gray Value: 100
Peak Right: Distance: 1.14-1.23, Avg. Gray Value: 100

- **For TiO_2 – Water with AA (Φ = 1.0%):**

Analysing the graph plot for TiO_2 – Water with Acetic Acid (AA) (Φ = 1.0%), it was noticed that there were many peaks along the line means the particles were distributed uniformly along the all area of the pattern. For the line at 0 degree with the origin (Fig. 40) Average Gray Value

was 180. For the line at 45 degree with the origin (Fig. 41) Average Gray Value was 180. For the line at 90 degree with the origin (Fig. 42) Average Gray Value was 180. For the line at 135 degree with the origin (Fig. 43) Average Gray Value was 180.

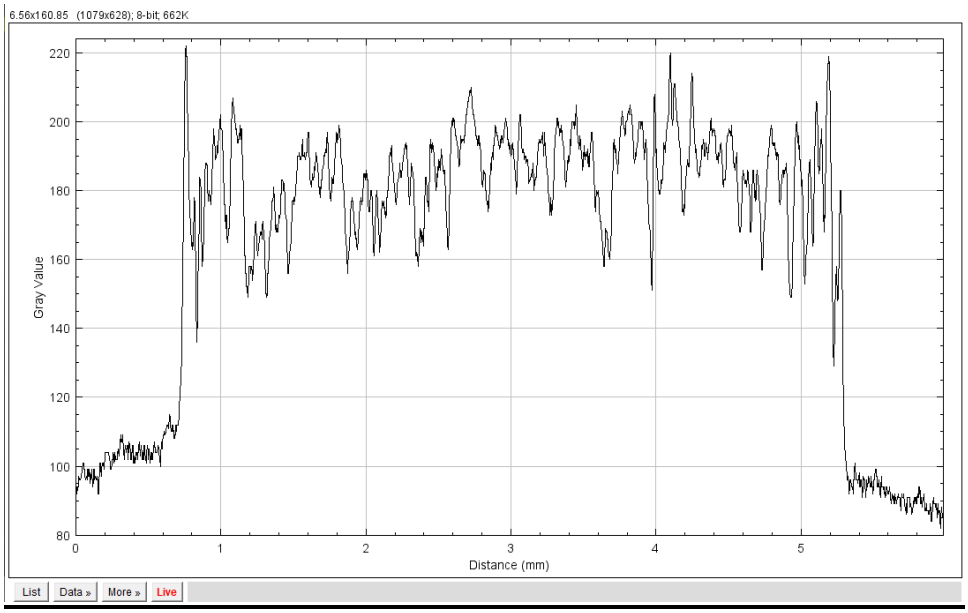

Fig 3.40: Gray Intensity Graph at 0 degree for TiO_2 – Water AA, Φ = 1.0
Avg. Gray Value for Uniform Distribution: 180

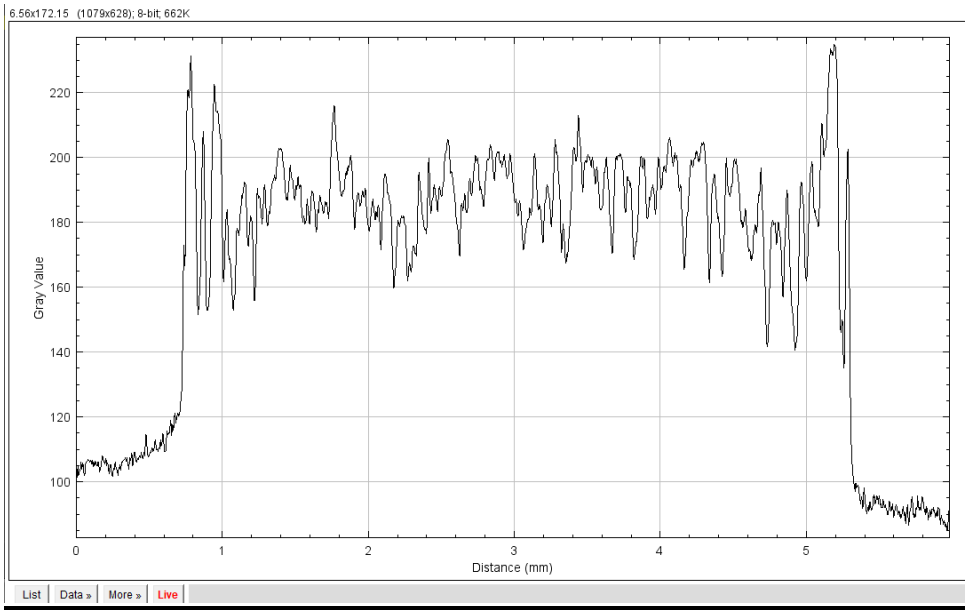

Fig 3.41: Gray Intensity Graph at 45 degree for TiO_2 – Water AA, Φ = 1.0
Avg. Gray Value for Uniform Distribution: 180

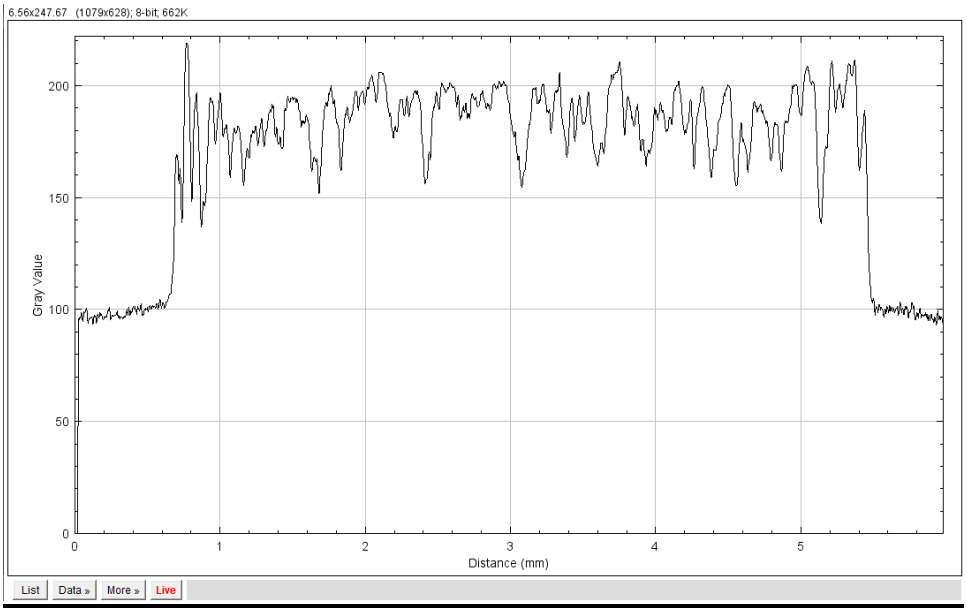

Fig 3.42: Gray Intensity Graph at 90 degree for TiO_2 – Water AA, Φ = 1.0
Avg. Gray Value for Uniform Distribution: 180

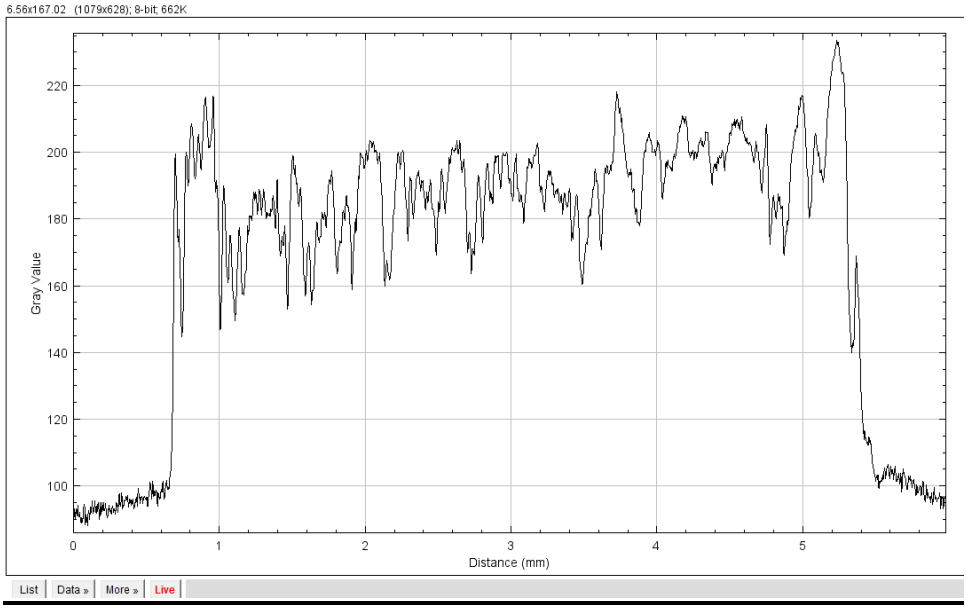

Fig 3.43: Gray Intensity Graph at 135 degree for TiO_2 – Water AA, Φ = 1.0
Avg. Gray Value for Uniform Distribution: 180

4. Conclusions and Future Direction:

4.1 Conclusions:

An experimental set up for the study of post-evaporation deposition pattern of nanofluid droplets was developed in house. Homogeneous and stable nanofluids were prepared from three types of nanoparticles such as TiO_2 in base fluid water for three different volume fractions such as Φ = 0.1%, Φ = 0.5% and Φ = 1.0%. Nanofluids samples were prepared following the Two-Step method and nanoparticles were sonicated in water in bath sonication method.

Different types of patterns were produced from the different nanofluid samples like coffee ring pattern, almost uniform patterns, hybrid patterns with coffee rings at the periphery and a gradient-deposit in the middle portion, etc.

- A clear coffee ring was produced from TiO_2-Water Nanofluid for volume fraction of $\Phi = 0.1\%$ and $\Phi = 0.5\%$, A uniform pattern was seen for TiO_2-Water Nanofluid for volume fraction of $\Phi = 1.0\%$
- With addition of surfactant (CTAB) there was a change in ring pattern, for volume fraction of $\Phi = 0.5\%$, a clean clear proper coffee ring was observed for TiO_2-Water Nanofluid with CTAB for volume fraction of $\Phi = 0.5\%$. and a very thin ring was seen for volume fraction of $\Phi = 1.0\%$.
- For TiO_2-Water Nanofluid with Acetic Acid (AA) a flower like structure was noticed for special condition for volume fraction $\Phi = 0.5\%$, and uniform structure was found for volume fraction $\Phi = 1.0\%$.
- For contact angle analysis it is observed that TiO_2-Water Nanofluid $\Phi = 0.1\%$, $\Phi = 0.5\%$ and $\Phi = 1.0\%$, there isn't much difference in angles. For TiO_2-Water Nanofluid with CTAB for volume fraction of $\Phi = 0.5\%$ and $\Phi = 1.0\%$, there was 2-3 degree of difference in left and right contact angle. For TiO_2-Water Nanofluid with Acetic Acid (AA) contact angle value was 3-4 degree higher for $\Phi = 0.5\%$ than $\Phi = 1.0\%$.
- For Gray Intensity Graph analysis periphery peak values were found as ring formation was seen in normal TiO_2-Water Nanofluid for volume fraction of $\Phi = 0.1\%$ and $\Phi = 0.5\%$. but uniform peak values for $\Phi = 1.0\%$. For TiO_2-Water Nanofluid with CTAB for volume fraction of $\Phi = 0.5\%$ periphery peak values were observed as well as uniform peak values in middle as there was small cluster of nanoparticles found in the middle after evaporation but for $\Phi = 1.0\%$ uniform distribution of peak values were noticed. For TiO_2-Water Nanofluid with Acetic Acid (AA) for volume fraction of $\Phi = 0.5\%$ periphery peak values as well as uniform peak values in middle were noticed, but for $\Phi = 1.0\%$ uniform distribution of peak values were observed.

4.2 Scope of Future Work:

Nanofluids were new class of fluid, it was used in many industrial and other applications. It also can be used in painting, printing, coating, surface patterning, etc. But it has high production cost and stability always has become a challenge to the researchers. Agglomeration and sedimentation occur after some hours of preparation of nanofluids. Adding some surfactant to the nanofluids sample can increase stability of nanofluids, so choosing proper surfactant and

selecting amount of surfactant were also a challenge to the researchers. Evaporation of a droplet was very common phenomenon in our daily life, but the mechanism of droplet evaporation was very complex. Scientists have done much study in the past decades on droplet post-evaporation pattern, morphology and crack formation and they tried to explain the produced physio-mechanical evaporation-driven flow. Still many opportunities and challenges remain in this field.

- The present study had to be truncated because of the lockdown in the face of the pandemic. Further work needs to be conducted on the study through dynamic light scattering (DLS) to identify the particle size distributions of the probe- and bath-sonicated nanofluid samples.
- High-resolution microscopy and scanning electron microscopy (SEM) need to be done to further resolve the particle cluster morphology on the deposits.
- To observe the evaporation of droplet in the external force fields like acoustic, electrostatic, magnetic, etc. These external force field could change induced flow and mass transfer during evaporation. Evaporation of droplet under acoustic levitation can suppress the coffee ring remarkably [76].
- Effect of flash-evaporation on the deposit pattern was another future extension of the present work.
- Evaporation of droplet in space station was also a very significant experiment. It will clarify the effect of gravity on induced convection flow and mass transfer during droplet evaporation.
- Effect of the substrate properties, e.g., its wettability, surface roughness, thermal diffusivity for different nanofluid composition can also be studied.
- Controlling the droplet post evaporation pattern like converting coffee ring patterns to uniform patterns and vice-versa was main challenge to the researchers. These deposited patterns were dependent on the particles volume fraction, addition of different surfactants, amount of surfactant etc. So many experiments were necessary to observe the effects of different variables and to use those in required application.

5. References:

[1] Zhong, Xin, Alexandru Crivoi, and Fei Duan. "Sessile nanofluid droplet drying." *Advances in colloid and interface science* 217 (2015): 13-30.

[2] Shimoni, Allon, Suzanna Azoubel, and Shlomo Magdassi. "Inkjet printing of flexible high-performance carbon nanotube transparent conductive films by "coffee ring effect"." *Nanoscale* 6.19 (2014): 11084-11089.

[3] Karatzas, Ioannis, and Steven E. Shreve. "Brownian motion." *Brownian Motion and Stochastic Calculus*. Springer, New York, NY, 1998. 47-127

[4] Wong, Kaufui V., and Omar De Leon. "Applications of nanofluids: current and future." *Advances in mechanical engineering* 2 (2010): 519659.

[5] Deegan, Robert D.; Bakajin, Olgica; Dupont, Todd F.; Huber, Greb; Nagel, Sidney R.; Witten, Thomas A. (1997). "Capillary flow as the cause of ring stains from dried liquid drops". Nature. 389 (6653): 827–829. Bibcode:1997, Natur.389..827D. doi:10.1038/39827. S2CID 205027233.

[6] Ooi, Yuto; Hanasaki, Itsuo; Mizumura, Daiki; Matsuda, Yu (2017). "Suppressing the coffee-ring effect of colloidal droplets by dispersed cellulose nanofibers". Science and Technology of Advanced Materials. 18 (1): 316–324. Bibcode:2017STAdM..18..316O. doi:10.1080/14686996.2017.1314776. PMC 5439399. PMID 28567177.

[7] Hu, H; Larson, R. G. (2006). "Marangoni Effect Reverses Coffee-Ring Depositions". *Journal of Physical Chemistry B*. **110** (14): 7090–7094. doi:10.1021/jp0609232. PMID 16599468.

[8] Savino, R.; Paterna, D.; Favaloro, N. (2002). "Buoyancy and Marangoni Effects in an Evaporating Drop". *Journal of Thermophysics and Heat Transfer*. **16** (4): 562–574. doi:10.2514/2.6716. ISSN 0887-8722.

[9] Jafari Kang, Saeed; Vandadi, Vahid; Felske, James D.; Masoud, Hassan (2016). "Alternative mechanism for coffee-ring deposition based on active role of free surface". *Physical Review E*. **94** (6):
063104. arXiv:0906.3878. Bibcode:2016PhRvE..94f3104J. doi:10.1103/PhysRevE.94.063104. PMID 28085318. S2CID 10670995.

[10] Coffee-ring phenomenon explained in new theory. phys.org (December 20, 2016)

[11] Gençer, Alican; Schütz, Christina; Thielemans, Wim (2017). "Influence of the Particle Concentration and Marangoni Flow on the Formation of Cellulose Nanocrystal Films". *Langmuir*. **33** (1): 228–234. doi:10.1021/acs.langmuir.6b03724. PMID 28034313.

[12] de Gans, Berend-Jan; Schubert, Ulrich S. (2004). "Inkjet Printing of Well-Defined Polymer Dots and Arrays". *Langmuir*. **20** (18): 7789–7793. doi:10.1021/la049469o. ISSN 0743-7463. PMID 15323532.

[13] Soltman, Dan; Subramanian, Vivek (2008). "Inkjet-Printed Line Morphologies and Temperature Control of the Coffee Ring Effect". *Langmuir*. **24** (5): 2224–2231. doi:10.1021/la7026847. ISSN 0743-7463. PMID 18197714.

[14] Patil, Nagesh D.; Bange, Prathamesh G.; Bhardwaj, Rajneesh; Sharma, Atul (2016). "Effects of Substrate Heating and Wettability on Evaporation Dynamics and Deposition Patterns for a Sessile Water Droplet Containing Colloidal Particles". *Langmuir*. **32** (45): 11958–
11972. arXiv:1610.06281. doi:10.1021/acs.langmuir.6b02769. PMID 27759960. S2CID 46708941.

[15] McBride, Samantha; Dash, Susmita; Varanasi, Kripa (2018). "Evaporative Crystallization in Drops on Superhydrophobic and Liquid-Impregnated Surfaces". *Langmuir*. **34** (41): 12350–12358. doi:10.1021/acs.langmuir.8b00049. hdl:1721.1/129769. PMID 29609465.

[16] Tan, Huanshu; Wooh, S.; Butt, H.-J.; Zhang, X.; Lohse, D. (2019). "Porous supraparticle assembly through self-lubricating evaporating colloidal ouzo drops". Nature Communications. 10 (1): 478. Bibcode:2019NatCo..10..478T. doi:10.1038/s41467-019-08385-w. PMC 6351649. PMID 30696829.

[17] Eral, H.B.; Mampallil-Augustine, D.; Duits, M.H.G.; Mugele, F. (2011). "Suppressing the

electrowetting". *Soft Matter*. **7** (10): 7090–7094. Bibcode:2011SMat....7.4954E. doi:10.1039/C1SM05183K.

[18] Weon, Byung Mook; Je, Jung Ho (2010). "Capillary force repels coffee-ring effect". *PhysicalReviewE*. **82** (1): 015305(R). Bibcode:2010PhRvE..82a5305W. doi:10.1103/PhysRevE.82.015305. PMID 20866682.

[19] Shen, X; Ho, C. M.; Wong, T. S. (2010). "Minimal Size of Coffee Ring Structure". *Journal of Physical Chemistry B*. **114** (16): 5269–5274. doi:10.1021/jp912190v. PMC 2902562. PMID 20353247.

[20] Yunker, P. J.; Still, T; Lohr, M. A.; Yodh, A. G. (2011). "Suppression of the coffee-ring effect by shape-dependent capillary interactions". *Nature*. **476** (7360): 308–311. Bibcode:2011Natur.476..308Y. doi:10.1038/nature10344. PMID 21850105. S2CID 205226009.

[21] "Coffee-ring effect explained". ScienceDebate.com. Retrieved 21 August 2011.

[22] Pack, Min; Hu, Han; Kim, Dong-Ook; Yang, Xin; Sun, Ying (2015). "Colloidal drop deposition on porous substrates: competition among particle motion, evaporation and infiltration". *Langmuir*. **31** (29): 7953–7961. doi:10.1021/acs.langmuir.5b01846. PMID 26132211.

[23] Bhardwaj, R; Fang, X; Somasundaran, P; Attinger, D (2010). "Self-Assembly of Colloidal Particles from Evaporating Droplets: Role of DLVO Interactions and Proposition of a Phase Diagram". *Langmuir*. **26** (11):7833-42. arXiv:1010.2564. doi:10.1021/la9047227. PMID 20337481. S2CID 4789514.

[24] P.J. Yunker, T. Still, M.A. Lohr, A.G. Yodh, Suppression of the coffee-ring effect by shape-dependent capillary interactions, Nature 476 (7360) (2011) 308–311,

[25] R. Bhardwaj, X. Fang, P. Somasundaran, D. Attinger, Self-assembly of colloidal particles from evaporating droplets: Role of DLVO interactions and proposition of a phase diagram, Langmuir 26 (11) (2010) 7833–7842,

[26] Maxwell, J. C. "Electricity and Magnetism Clarendon Press." (1873). 6Masuda, Hidetoshi, et al. "Alteration of thermal conductivity and viscosity of liquid by dispersing ultra-fine particles (dispersion of γ-Al2O3, SiO2 and TiO2 ultra-fine particles)." (1993).

[27] Deegan, Robert D., et al. "Capillary flow as the cause of ring stains from dried liquid drops." *Nature* 389.6653 (1997): 827-829.

[28] R.D. Deegan, O. Bakajin, T.F. Dupont, G. Huber, S.R. Nagel, T.A. Witten, Capillary flow as the cause of ring stains from dried liquid drops, Nature 389 (6653) (1997) 827–829,

[29] D. Orejon, K. Sefiane, M.E.R. Shanahan, Stick–slip of evaporating droplets: Substrate hydrophobicity and nanoparticle concentration, Langmuir 27 (21) (2011) 12834–12843,

[30] Shen, Xiaoying, Chih-Ming Ho, and Tak-Sing Wong. "Minimal size of coffee ring structure." *The Journal of Physical Chemistry B* 114.16 (2010): 5269-5274.

[31] Nguyen, Tuan AH, and Anh V. Nguyen. "Increased evaporation kinetics of sessile droplets by using nanoparticles." *Langmuir* 28.49 (2012): 16725-16728.

[32] Shimoni, Allon, Suzanna Azoubel, and Shlomo Magdassi. "Inkjet printing of flexible high-performance carbon nanotube transparent conductive films by “coffee ring effect”." *Nanoscale* 6.19 (2014): 11084-11089.

[33] Wong, Tak-Sing, et al. "Nano chromatography driven by the coffee ring effect." *Analytical chemistry* 83.6 (2011): 1871-1873.